Naturally enhanced neutralizing breadth to SARS-CoV-2 after one year

Zijun Wang[1,*], Frauke Muecksch[2,*], Dennis Schaefer-Babajew[1,*], Shlomo Finkin[1,*], Charlotte Viant[1,*], Christian Gaebler[1,*], Hans- Heinrich Hoffmann[3], Christopher O. Barnes[4], Melissa Cipolla[1], Victor Ramos[1], Thiago Y. Oliveira[1], Alice Cho[1], Fabian Schmidt[2], Justin da Silva[2], Eva Bednarski[2], Lauren Aguado[3], Jim Yee[5], Mridushi Daga[1], Martina Turroja[1], Katrina G. Millard[1], Mila Jankovic[1], Anna Gazumyan[1, 6], Zhen Zhao[5], Charles M. Rice[3], Paul D. Bieniasz[2, 6], Marina Caskey[1], Theodora Hatziioannou[2], Michel C. Nussenzweig[1, 6]

[1]Laboratory of Molecular Immunology, The Rockefeller University, New York, NY 10065, USA

[2]Laboratory of Retrovirology, The Rockefeller University, New York, NY 10065, USA

[3]Laboratory of Virology and Infectious Disease, The Rockefeller University, New York, NY, 10065, USA.

[4]Division of Biology and Biological Engineering, California Institute of Technology, Pasadena, CA, USA.

[5]Department of Pathology and Laboratory Medicine, Weill Cornell Medicine, New York, NY, 10065, USA

[6]Howard Hughes Medical Institute

*equal contribution

Address correspondence to: Paul D. Bieniasz, pbieniasz@rockefeller.edu; Marina Caskey, mcaskey@rockefeller.edu; Theodora Hatziioannou, thatziio@rockefeller.edu; or Michel C. Nussenzweig, nussen@rockefeller.edu.

Over one year after its inception, the coronavirus disease-2019 (COVID-19) pandemic caused by severe acute respiratory syndrome coronavirus-2 (SARS-CoV-2) remains difficult to control despite the availability of several excellent vaccines. Progress in controlling the pandemic is slowed by the emergence of variants that appear to be more transmissible and more resistant to antibodies[1,2]. Here we report on a cohort of 63 COVID-19-convalescent individuals assessed at 1.3, 6.2 and 12 months after infection, 41% of whom also received mRNA vaccines[3,4]. In the absence of vaccination antibody reactivity to the receptor binding domain (RBD) of SARS-CoV-2, neutralizing activity and the number of RBD-specific memory B cells remain relatively stable from 6 to 12 months. Vaccination increases all components of the humoral response, and as expected, results in serum neutralizing activities against variants of concern that are comparable to or greater than neutralizing activity against the original Wuhan Hu-1 achieved by vaccination of naïve individuals[2,5-8]. The mechanism underlying these broad-based responses involves ongoing antibody somatic mutation, memory B cell clonal turnover, and development of monoclonal antibodies that are exceptionally resistant to SARS-CoV-2 RBD mutations, including those found in variants of concern[4,9]. In addition, B cell clones expressing broad and potent antibodies are selectively retained in the repertoire over time and expand dramatically after vaccination. The data suggest that immunity in convalescent individuals

will be very long lasting and that convalescent individuals who receive available mRNA vaccines will produce antibodies and memory B cells that should be protective against circulating SARS-CoV-2 variants.

We initially characterized immune responses to SARS-CoV-2 in a cohort of convalescent individuals 1.3 and 6.2 months after infection[3,4]. Between February 8 and March 26, 2021, 63 participants between the ages of 26 and 73 years old (median 47 years) returned for a 12-month follow-up visit. Among those, 26 (41%) had received at least one dose of either the Moderna (mRNA-1273) or Pfizer-BioNTech (BNT162b2) vaccines, on average 40 days (range 2-82 days) before their study visit and 311 days (range 272-373 days) after onset of acute illness (Supplementary Table 1). Participants were was almost evenly split between sexes (43% female) and of the individuals that returned for a 12-month follow-up, only 10% had been hospitalized and the remainder had experienced relatively mild initial infections. Only 14% of the individuals reported persistent long-term symptoms after 12 months, reduced from 44% at the 6-month time point[4]. Symptom persistence was not associated with the duration and severity of acute disease or with vaccination status (Extended Data Fig. 1 a-c). All participants tested negative for active infection at the 12-month time point as measured by a saliva-based PCR assay [4]. The demographics and clinical characteristics of the participants are shown in Supplementary Tables 1 and 2.

Plasma SARS-CoV-2 Antibody Reactivity

Antibody reactivity in plasma to the RBD and nucleoprotein (N) were measured by enzyme-linked immunosorbent assay (ELISA)[3]. We limited our analysis to RBD because plasma anti-

70 RBD antibodies are strongly correlated with neutralizing activity [3,10-12]. Convalescent
71 participants who had not been vaccinated maintained most of their anti-RBD IgM (103%), IgG
72 (82%), and IgA (72%) titers between 6 and 12 months (Fig. 1a and Extended Data Fig. 2a-k).
73 Consistent with previous reports[5-8], vaccination increased the anti-RBD plasma antibody levels,
74 with IgG titers increasing by nearly 30-fold compared to unvaccinated individuals (Fig. 1a right).
75 The 2 individuals who did not show an increase had been vaccinated only 2 days before sample
76 collection. In contrast to anti-RBD antibody titers that were relatively stable, anti-N antibody
77 titers decreased significantly between 6 and 12 months in this assay irrespective of vaccination
78 (Fig. 1b and Extended Data Fig. 2l-n).
79
80 Plasma neutralizing activity in 63 participants was measured using an HIV-1 pseudotyped with
81 the SARS-CoV-2 spike protein [3,4,13] (Fig. 1c-d and Extended Data Fig. 2o). Twelve-months after
82 infection, the geometric mean half-maximal neutralizing titer (NT_{50}) for the 37 individuals that
83 had not been vaccinated was 75, which was not significantly different from the same individuals
84 at 6.2 months (Fig. 1c). In contrast, the vaccinated individuals showed a geometric mean NT_{50} of
85 3,684, which was nearly 50-fold greater than unvaccinated individuals and slightly better
86 compared to the 30-fold increase in anti-RBD IgG antibodies (Fig. 1a, c, and d). Neutralizing
87 activity was directly correlated with IgG anti-RBD (Extended Data Fig.2p) but not with anti-N
88 titers (Extended Data Fig.2r). We conclude that neutralizing titers remain relatively unchanged
89 between 6 to 12 months after SARS-CoV-2 infection, and that vaccination further boosts this
90 activity by nearly 50-fold.
91

92 To determine the neutralizing activity against circulating variants of concern/interest, we
93 performed neutralization assays on HIV-1 virus pseudotyped with the S protein of the following
94 SARS-CoV-2 variants of concern/interest: B.1.1.7, B.1.351, B.1.526 and P.1 [1,14,15]. Twelve-
95 months after infection neutralizing activity against the variants was generally lower than against
96 wild-type SARS-CoV-2 virus in the same assay with the greatest loss of activity against B.1.351
97 (Fig. 1e). After vaccination the geometric mean NT_{50} rose to 11,493, 48,341, 22,109 and 26,553
98 against B.1.351, B.1.1.7, B.1.526 and P.1, respectively. These titers are an order of magnitude
99 higher than the neutralizing titers we and others have reported against the wild-type SARS-CoV-
100 2 at the peak of the initial response in infected individuals and in naïve individuals receiving both
101 doses of mRNA vaccines (Fig. 1d and [2-8]). Similar results were also obtained using authentic
102 SARS-CoV-2 WA1/2020 and B.1.351 (Extended Data Fig.2s).
103
104 **Memory B cells**
105 The memory B cell compartment serves as an immune reservoir that contains a diverse collection
106 of antibodies[16,17]. Although antibodies to the N-terminal domain and other parts of S can also be
107 neutralizing, we limited our analysis to memory B cells that produce anti-RBD antibodies
108 because they are the most numerous and potent [18,19]. To enumerate RBD-specific memory B
109 cells, we performed flow cytometry using a biotin-labeled RBD[3] (Fig. 2a and Extended Data Fig.
110 3a and b). In the absence of vaccination, the number of RBD specific memory B cells present at
111 12 months was only 1.35-fold lower than the earlier timepoint (p= 0.027, Fig. 2a). In contrast
112 and consistent with previous reports[5,8,20], convalescent individuals that received mRNA vaccines
113 showed an average 8.6-fold increase in the number of circulating RBD specific memory B cells
114 (Fig. 2a). B cells expressing antibodies that bound to both wild-type and K417N/E484K/N501Y

115 mutant RBDs were also enumerated by flow cytometry (Extended Data Fig. 3c). The number of
116 variant RBD cross-reactive B cells was directly proportional to but 1.6 to 3.2-fold lower than
117 wild-type RBD binding B cells (Fig. 2a).
118
119 The memory B cell compartment accumulates mutations and undergoes clonal evolution over the
120 initial 6 months after infection[4,9,21,22]. To determine whether the memory compartment continues
121 to evolve between 6 and 12 months, we obtained 1105 paired antibody heavy and light chain
122 sequences from 10 individuals that were also assayed at the earlier time points, 6 of which were
123 vaccinated (Fig. 2b, Extended Data Fig 3d, Supplementary Table 3). There were few significant
124 differences among the expressed IGHV and IGLV genes between vaccinated and un-vaccinated
125 groups, or between the 1.3-, 6-month and 1 year time points (Extended Data Fig 4a-c)[3,4]. *IGHV3-*
126 *30* and *IGHV3-53* remained over-represented irrespective of vaccination [10,18](Extended Data Fig
127 4a).
128
129 All individuals assayed at 12 months showed expanded clones of RBD-binding memory cells
130 that expressed closely related IGHV and IGLV genes (Fig.2b, Extended Data Fig 3d and e). The
131 relative fraction of cells belonging to these clones varied from 7-54% of the repertoire with no
132 significant difference between vaccinated and non-vaccinated groups. The overall clonal
133 composition differed between 6 and 12 months in all individuals suggesting ongoing clonal
134 evolution (Fig. 2b and Extended Data Fig 3d). Among the 89 clones found after 12 months, 61%
135 were not previously detected and 39% were present at one of the earlier time points (Fig. 2b and
136 Extended Data Fig 3d). In vaccinated individuals the increase in size of the memory
137 compartment was paralleled by an increase in the absolute number of B cells representing all

138 persistent clones (Extended Data Fig 5a). Thus, RBD specific memory B cell clones were re-
139 expanded upon vaccination in all 6 convalescent individuals examined (Fig. 2b and Extended
140 Data Fig 3d and Extended Data Fig 5a).
141
142 Somatic hypermutation of antibody genes continued between 6 and 12 months after infection
143 (Fig. 2c). Slightly higher levels of mutation were found in individuals who had not been
144 vaccinated compared to vaccinated individuals possibly due to recruitment of newly-formed
145 memory cells into the expanded memory compartment of the vaccinated individuals (Fig. 2c,
146 Extended Data Fig 5b). There was no significant difference in mutation between conserved and
147 newly arising clones at the 12-month time point in vaccinated individuals (Extended Data Fig
148 5c). Moreover, phylogenetic analysis revealed that sequences found at 6 and 12 months were
149 intermingled and similarly distant from their unmutated common ancestors (Extended Data Fig
150 6). We conclude that clonal re-expansion of memory cells in response to vaccination is not
151 associated with additional accumulation of large numbers of somatic mutations as might be
152 expected if the clones were re-entering and proliferating in germinal centers.
153
154 **Neutralizing Activity of Monoclonal Antibodies**
155 To determine whether the antibodies obtained from memory B cells 12 months after infection
156 bind to RBD we performed ELISAs (Fig.3a). 174 antibodies were tested by ELISA including: 1.
157 53 that were randomly selected from those that appeared only once and only after 1 year; 2. 91
158 that appeared as expanded clones or singlets at more than one time point; 3. 30 representatives of
159 newly arising expanded clones (Supplementary Tables 4 and 5). Among the 174 antibodies
160 tested, 173 bound to RBD indicating that the flow cytometry method used to identify B cells

161 expressing anti-RBD antibodies was efficient (Supplementary Tables 4 and 5). The geometric
162 mean ELISA half-maximal concentration (EC_{50}) of the antibodies obtained after 12 months was
163 2.6 ng/ml, which was significantly lower than at 6 months irrespective of vaccination and
164 suggestive of an increase in affinity (Fig. 3a, Extended data Fig. 7 a and b and Supplementary
165 Tables 4 and 5). Consistent with this observation there was an overall increase in the apparent
166 avidity of plasma antibodies between 1.3 and 12 months [3,4]($p<0.0001$, Extended data Fig. 7c).
167
168 All 174 RBD binding antibodies obtained from the 12-month time point were tested for
169 neutralizing activity in a SARS-CoV-2 pseudotype neutralization assay. When compared to the
170 earlier time points from the same individuals, the geometric mean half maximal inhibitory
171 concentration (IC_{50}) improved from 171 ng/mL (1.3 months) to 116 ng/mL (6 months) to 79
172 ng/mL (12 months), with no significant difference between vaccinated and non-vaccinated
173 individuals (Fig. 3b and Extended data Fig. 7d, Supplementary Table 4). The increased potency
174 was especially evident in the antibodies expressed by expanded clones of B cells that were
175 conserved for the entire observation period irrespective of vaccination ($p=0.014$, Fig. 3b right,
176 Extended Data Fig 7e-h and Supplementary Table 5). The overall increase in neutralizing
177 activity among conserved clones was due to accumulation of clones expressing antibodies with
178 potent neutralizing activity and simultaneous loss of clones expressing antibodies with no
179 measurable activity ($p= 0.028$, Fig 3b right pie charts). Consistent with this observation,
180 antibodies obtained from clonally expanded B cells after 12 months were more potent than
181 antibodies obtained from unique B cells at the same time point ($p= 0.029$, Fig 3b).
182
183 **Epitopes and Breadth of Neutralization**

184 To determine whether the loss of non-neutralizing antibodies over time was due to preferential
185 loss of antibodies targeting specific epitopes, we performed BLI experiments in which a
186 preformed antibody-RBD complex was exposed to a second monoclonal targeting one of 3
187 classes of structurally defined epitopes[3,23] (see schematic in Fig. 4a). We assayed 60 randomly
188 selected antibodies with comparable neutralizing activity from the 1.3- and 12-month time
189 points. The 60 antibodies were evenly distributed between the 2 time points and between
190 neutralizers and non-neutralizers (Fig. 4). Antibody affinities for RBD were similar among
191 neutralizers and non-neutralizers obtained at the same time point (Fig. 4b, Extended Data Fig. 8).
192 When the two sets of un-related antibodies obtained from 1.3 and 12 months were compared,
193 they showed significantly increased affinity over time irrespective of their neutralizing activity
194 (Fig. 4b, Extended Data Fig. 8). In competition experiments, all but 2 of the 30 non-neutralizing
195 antibodies failed to inhibit binding of the class 1 (C105), 2 (C121 and C144) or 3 (C135)
196 antibodies tested and therefore must bind to epitopes that do not overlap with the epitopes of
197 these classes of antibodies (Fig. 4c, and Extended Data Fig. 9). In contrast, all but 2 of the 30
198 neutralizers blocked class 1, or 2 antibodies whose target epitopes are structural components of
199 the RBD that interact with its cellular receptor, the angiotensin-converting enzyme 2[23,24] (ACE2)
200 (Fig. 4c and Extended Data Fig. 9). In addition, whereas 9 of the 15 neutralizing antibodies
201 obtained after 1.3 months blocked both class 1 and 2 antibodies, only 1 of the 15 obtained after
202 12 months did so. In contrast to the earlier time point, 13 of 15 neutralizing antibodies obtained
203 after 12 months only interfered with C121, a class 2 antibody[3,23] (Fig. 4c and Extended Data Fig.
204 9). We conclude that neutralizing antibodies are retained and non-neutralizing antibodies
205 targeting RBD surfaces that do not interact with ACE2 are removed from the repertoire over
206 time.

207

208 To determine whether there was an increase in neutralization breadth over time, the neutralizing
209 activity of the 60 antibodies was assayed against a panel of RBD mutants covering residues
210 associated with circulating variants of concern: R346S, K417N, N440K, A475V, E484K and
211 N501Y (Fig. 4d and Supplementary Table 6). Increased activity was evident against K417N,
212 N440K, A475V, E484K and N501Y (Fig. 4d and Supplementary Table 6). We conclude that
213 evolution of the antibody repertoire results in acquisition of neutralization breadth over time.

214

215 The increase in breadth and overall potency of memory B cell antibodies could be due to shifts in
216 the repertoire, clonal evolution, or both. To determine whether changes in specific clones are
217 associated with increases in affinity and breadth, we measured the relative affinity and
218 neutralizing breadth of matched pairs of antibodies expressed by expanded clones of B cells that
219 were maintained in the repertoire over the entire observation period[3,4]. SARS-CoV-2 neutralizing
220 activity of the antibodies present at 1.3 or 12 months was not significantly correlated with
221 affinity at either time point when each time point is considered independently (Fig. 4e).
222 However, there was a significant increase in overall affinity over time including in the 4 pairs of
223 antibodies with no measurable neutralizing activity (Fig. 4f and Supplementary Table 7).
224 Neutralizing breadth was assayed for 15 randomly selected pairs of antibodies targeting epitopes
225 assigned to the 3 dominant classes of neutralizing antibodies[3,23,25,26]. Seven of the selected
226 antibodies showed equivalent or decreased activity against wild-type SARS-CoV-2 after 12
227 months (Fig. 4g and Supplementary Table 8). However, neutralizing breadth increased between
228 1.3 and 12-months for all 15 pairs, even when neutralizing activity against the wild-type was
229 unchanged or decreased (Fig. 4g and Supplementary Table 8). Only 1 of the 15 antibodies

230 obtained after 1.3 months neutralized all the mutants tested (Fig. 4g). In contrast, 10 of the 15
231 antibodies obtained from the same clones after 12 months neutralized all variants tested with
232 IC_{50}s as low as 1 ng/ml against the triple mutant K417N/E484K/N501Y found in B.1.351 (Fig.
233 4g and Supplementary Table 8). Similar results were obtained with authentic WA1/2020 and
234 B.1.351 (Extended Data Fig 7i). In conclusion, continued clonal evolution of anti-SARS-CoV-2
235 antibodies over 12 months favors increasing potency and breadth resulting in monoclonal
236 antibodies with exceptional activity against a broad group of variants.
237
238 **Discussion**
239 During immune responses activated B cells interact with cognate T cells and begin dividing
240 before selection into the plasma cell, memory or germinal center B cell compartments based in
241 part on their affinity for antigen[17,27-31]. Whereas B cells expressing high affinity antibodies are
242 favored to enter the long-lived plasma cell compartment, the memory compartment is more
243 diverse and can develop directly from activated B cells or from a germinal center[17,27-31].
244 Memory cells emanating from a germinal center carry more mutations than those that develop
245 directly from activated B cells because they undergo additional cycles of division[32].
246
247 Consistent with the longevity of bone marrow plasma cells, infection with SARS-CoV-2 leads to
248 persistent serum anti-RBD antibodies, and corresponding neutralizing responses. Nearly 93% of
249 the plasma neutralizing activity is retained between 6- and 12-months[33,34]. Vaccination boosts the
250 neutralizing response by 1.5 orders of magnitude by inducing additional plasma cell
251 differentiation from the memory B cell compartment [5,7,35]. Recruitment of evolved memory B
252 cells producing antibodies with broad and potent neutralizing activity into the plasma cell

253 compartment is likely to account for the exceptional serologic activity of vaccinated
254 convalescents against variants of concern[20,35,36].
255
256 Less is known about selection and maintenance of the memory B cell compartment. SARS-CoV-
257 2 infection produces a memory compartment that continues to evolve over 12 months after
258 infection with accumulation of somatic mutations, emergence of new clones, and increasing
259 affinity all of which is consistent with long-term persistence of germinal centers. The increase in
260 activity against SARS-CoV-2 mutants parallels the increase in affinity and is consistent with the
261 finding that increasing the apparent affinity of anti-SARS-CoV-2 antibodies by dimerization or
262 by creating bi-specific antibodies also increases resistance to RBD mutations[37-40].
263
264 Continued antibody evolution in germinal centers requires antigen which can be retained in these
265 structures over long periods of time[29]. In addition, SARS-CoV-2 protein and nucleic acid has
266 been reported in the gut for at least 2 months after infection[4]. Irrespective of the source of
267 antigen, antibody evolution favors epitopes overlapping with the ACE2 binding site on the RBD,
268 possibly because these are epitopes that are preferentially exposed on trimeric spike protein or
269 virus particles.
270
271 Vaccination after SARS-CoV-2 infection increases the number of RBD binding memory cells by
272 over an order of magnitude by recruiting new B cell clones into memory and expanding
273 persistent clones. The persistent clones expand without accumulating large numbers of additional
274 mutations indicating that clonal expansion of human memory B cells does not require re-entry
275 into germinal centers and occurs through the activated B cell compartment[17,27-31].

The remarkable evolution of breadth after infection and the robust enhancement of serologic responses and B cell memory achieved with mRNA vaccination suggests that convalescent individuals who are vaccinated should enjoy high levels of protection against emerging variants without a need to modify existing vaccines. If memory responses evolve in a similar manner in naive individuals that receive vaccines, additional appropriately timed boosting with available vaccines should lead to protective immunity against circulating variants.

Figures

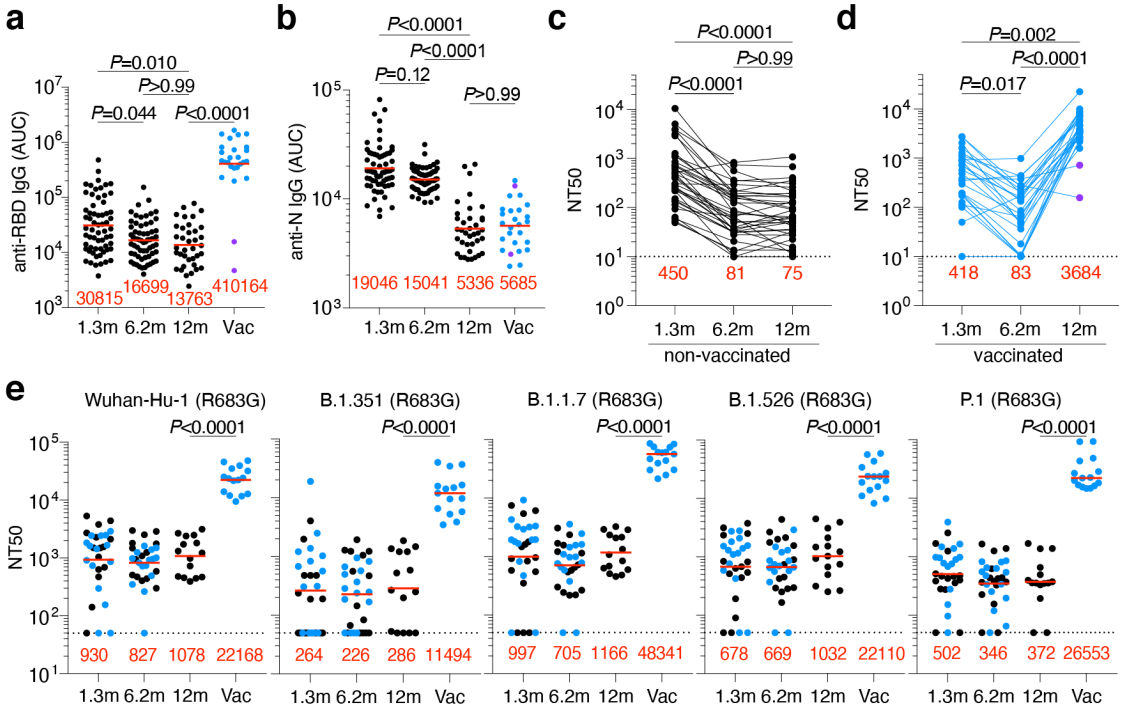

289 **Fig. 1: Plasma ELISAs and neutralizing activity. a-b,** Plasma IgG antibody binding to SARS-
290 CoV-2 RBD (**a**) and N protein (**b**), and plasma neutralizing activity (**c**–**d**) 12 months after infection
291 (n=63). **a** and **b**, Area under the curve (AUC) over time in non-vaccinated and vaccinated
292 individuals, as indicated. Numbers in red indicate geometric mean AUC at the indicated timepoint.
293 n=63, 37 convalescent and 26 convalescent vaccinated individuals. Statistical significance in **a** and
294 **b** was determined using two-sided Kruskal-Wallis test with subsequent Dunn's multiple
295 comparisons. **c, d,** NT50 over time in non-vaccinated (**c**) and vaccinated individuals (**d**). Lines
296 connect longitudinal samples from the same individual. Statistical significance in **c-d** was
297 determined using two-sided Friedman test with subsequent Dunn's multiple comparisons. Two
298 individuals who received their first dose of vaccine 24-48 hours before sample collection are
299 depicted in purple. **e**, Plasma neutralizing activity against indicated SARS-CoV-2 variants of
300 concern (n=30, 15 convalescent and 15 convalescent vaccinated individuals). The B.1.526 variant
301 used here does contain the E484K substitution. Please refer to Methods for a detailed list of all
302 substitutions/deletions/insertions of spike variants used here. Convalescent and convalescent
303 vaccinated individuals in **a-e** are shown in black and blue, respectively. Statistical significance was
304 determined using two-tailed Mann-Whitney test. Red numbers in c-e indicate the geometric mean
305 NT50 at the indicated timepoint. All experiments were performed at least in duplicate.
306

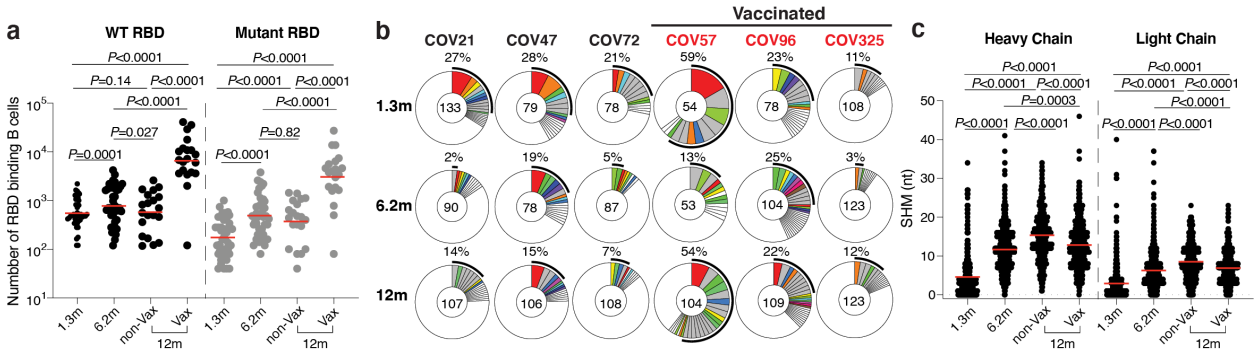

Fig. 2: Anti-SARS-CoV-2 RBD B cell memory. a, graph summarizes number of antigen binding memory B cells per 2 million B cells (Extended data Fig 5b and c) obtained at 1.3, 6.2 and 12 months from 40 randomly selected individuals (vaccinees n=20, and non-vaccinees, n=20). Each dot is one individual. Red horizontal bars indicate geometric mean values. Statistical significance was determined using two-sided Kruskal-Wallis test with subsequent Dunn's multiple comparisons. **b,** Pie charts show the distribution of antibody sequences from 6 individuals after 1.3 [3] (upper panel) or 6.2 [4] (middle panel) or 12 months (lower panel). The number in the inner circle indicates the number of sequences analyzed for the individual denoted above the circle. Pie slice size is proportional to the number of clonally related sequences. The black outline indicates the frequency of clonally expanded sequences detected in each participant. Colored slices indicate persisting clones (same IGV and IGJ genes, with highly similar CDR3s) found at both timepoints in the same participant. Grey slices indicate clones unique to the timepoint. White indicates sequences isolated once, and white slices indicate singlets found at both timepoints. **c.** Number of somatic nucleotide mutations in the IGVH and IGVL in antibodies (also Supplementary table 3) obtained after 1.3 or 6.2 or 12 months (1.3m: n=889; 6.2m: n=975; 12m: n=1105, (non-vax: n=417; vax: n=688)). Red horizontal bars indicate mean values. Statistical significance was determined using two-sided Kruskal-Wallis test with subsequent Dunn's multiple comparisons.

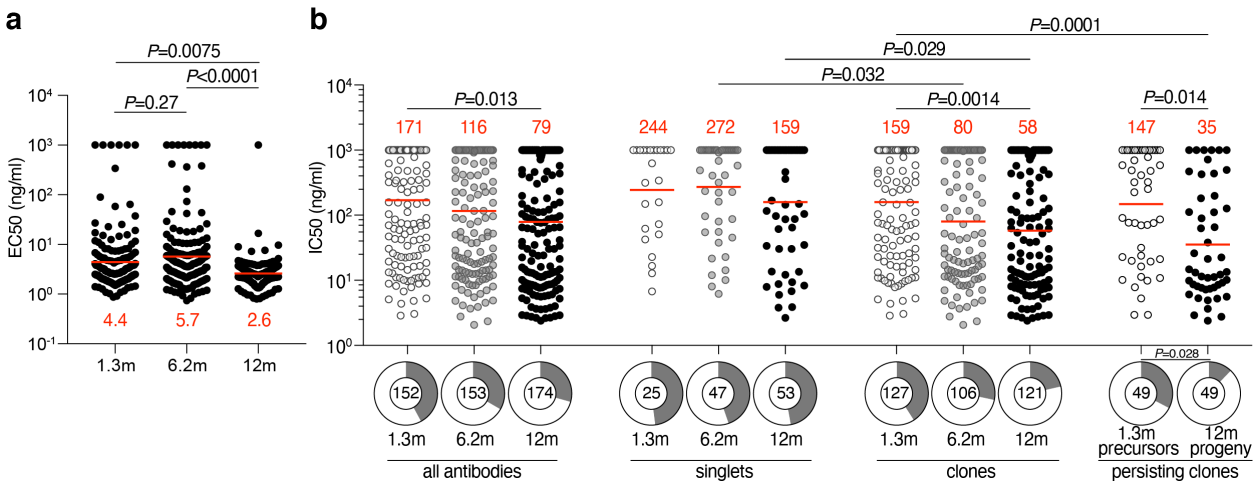

Fig. 3: Anti-SARS-CoV-2 RBD monoclonal antibodies. a, Graph shows the ELISA binding EC_{50} (Y axis) for SARS-CoV-2 RBD by antibodies isolated at 1.3[3] (n=152) 6.2[4] (n=153) and 12 months (n=174) after infection. Statistical significance was determined using the two-sided Kruskal-Wallis test with subsequent Dunn's multiple comparisons (1.3 vs 6.2 months, p=0.27; 1.3 vs 12 months, p=0.0075; 6.2 vs 12 months, p<0.0001). **b,** Graph shows anti-SARS-CoV-2 neutralizing activity of monoclonal antibodies measured by a SARS-CoV-2 pseudovirus neutralization assay[3,13]. Half-maximal inhibitory concentration (IC_{50}) values for antibodies isolated at 1.3[3] 6.2[4] and 12 months after infection against wild-type SARS-CoV-2 (Wuhan-Hu-1 strain[41]) are shown. Each dot represents one antibody. Pie charts illustrate the fraction of non-neutralizing (IC50 > 1000 ng/ml) antibodies (grey slices), inner circle shows the number of antibodies tested per group. Horizontal bars and red numbers indicate geometric mean values. Statistical significance was determined through the two-sided Kruskal Wallis test with subsequent Dunn's multiple comparisons.

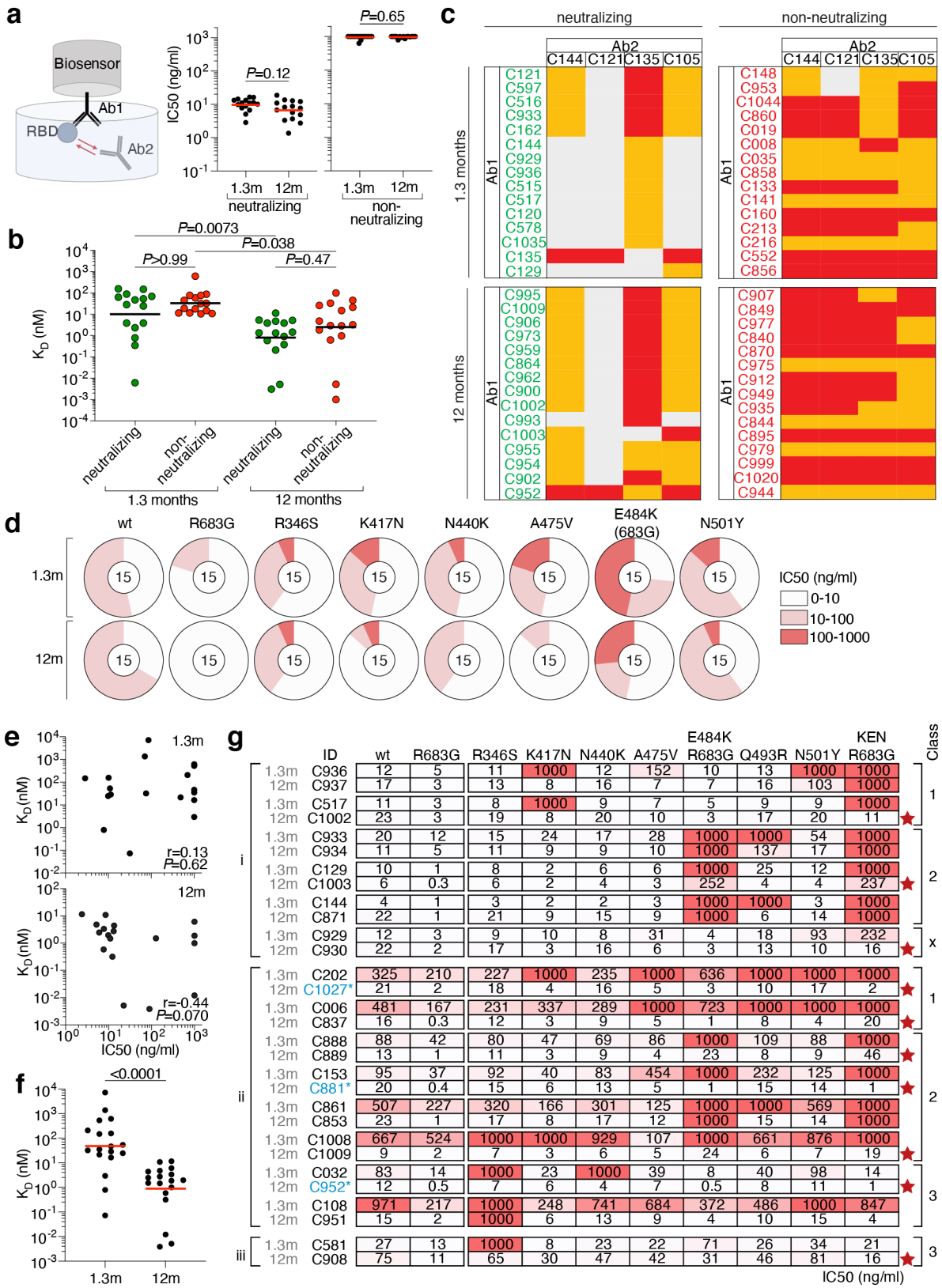

		ID	wt	R683G	R346S	K417N	N440K	A475V	E484K R683G	Q493R	N501Y	KEN R683G	Class
i	1.3m	C936	12	5	11	1000	12	152	10	13	1000	1000	1
	12m	C937	17	3	13	8	16	7	7	16	103	1000	
	1.3m	C517	11	3	8	1000	9	7	5	9	9	1000	
	12m	C1002	23	3	19	8	20	10	3	17	20	11 ★	
	1.3m	C933	20	12	15	24	17	28	1000	1000	54	1000	2
	12m	C934	11	5	11	9	9	10	1000	137	17	1000	
	1.3m	C129	10	1	8	2	6	6	1000	25	12	1000	
	12m	C1003	6	0.3	6	2	4	3	252	4	4	237 ★	
	1.3m	C144	4	1	3	2	2	3	1000	1000	3	1000	
	12m	C871	22	1	21	9	15	9	1000	6	14	1000	
	1.3m	C929	12	3	9	10	8	31	4	18	93	232	x
	12m	C930	22	2	17	3	16	6	3	13	10	16 ★	
ii	1.3m	C202	325	210	227	1000	235	1000	636	1000	1000	1000	1
	12m	C1027*	21	2	18	4	16	5	3	10	17	2 ★	
	1.3m	C006	481	167	231	337	289	1000	723	1000	1000	1000	
	12m	C837	16	0.3	12	3	9	5	1	8	4	20 ★	
	1.3m	C888	88	42	80	47	69	86	1000	109	88	1000	2
	12m	C889	13	1	11	3	9	4	23	8	9	46 ★	
	1.3m	C153	95	37	92	40	83	454	1000	232	125	1000	
	12m	C881*	20	0.4	15	6	13	5	1	15	14	1 ★	
	1.3m	C861	507	227	320	166	301	125	1000	1000	569	1000	
	12m	C853	23	1	17	8	17	12	1000	15	14	1000	
	1.3m	C1008	667	524	1000	1000	929	107	1000	661	876	1000	
	12m	C1009	9	2	7	3	6	5	24	6	7	19 ★	
	1.3m	C032	83	14	1000	23	1000	39	8	40	98	14	3
	12m	C952*	12	0.5	7	6	4	7	0.5	8	11	1 ★	
	1.3m	C108	971	217	1000	248	741	684	372	486	1000	847	
	12m	C951	15	2	1000	6	13	9	4	10	15	4	
iii	1.3m	C581	27	13	1000	8	23	22	71	26	34	21	3
	12m	C908	75	11	65	30	47	42	31	46	81	16 ★	

342 **Fig. 4: Epitope targeting and evolution of anti-SARS-CoV-2 RBD antibodies. a**, Schematic
343 representation of the BLI experiment (left) and IC_{50} values for randomly selected neutralizing
344 (middle) and non-neutralizing (right) antibodies isolated at 1.3- and 12-months post-infection
345 (each presented group shows n=15 antibodies, resulting in a total of n=60 antibodies). Red
346 horizontal bars indicate geometric mean. Statistical significance was determined using two-sided
347 Mann-Whitney test. **b**, K_D values of the n=30 neutralizing (green) and n=30 non-neutralizing (red)
348 antibodies shown in a. Horizontal bars indicate geometric mean values. Statistical significance was
349 determined using two-sided Kruskal Wallis test with subsequent Dunn's multiple comparisons.
350 BLI traces can be found in Extended data Fig. 8. **c,** Heat-map of relative inhibition of Ab2 binding
351 to the preformed Ab1-RBD complexes (grey=no binding, orange=intermediate binding, red=high
352 binding). Values are normalized through the subtraction of the autologous antibody control. BLI
353 traces can be found in Extended Data Fig 9. **d**, Neutralization of the indicated mutants for
354 antibodies shown in panel **a-c**. Pie charts illustrate the fraction of antibodies that are poorly/non-
355 neutralizing (IC_{50} 100-1000 ng/ml, red), intermediate neutralizing (IC_{50} 10-100 ng/ml, pink) and
356 potently neutralizing (IC_{50} 0-10 ng/ml, white) for each mutant. Number in inner circle shows
357 number of antibodies tested. **e,** Graphs show affinities (Y axis) plotted against neutralization
358 activity (X axis) for 18 clonal antibody pairs isolated 1.3 (top) and 12 months (bottom) (after
359 infection (n=36 antibodies). Statistical significance was determined using Spearman correlation
360 test. **f,** BLI affinity measurements for same n=36 paired 1.3- and 12-month antibodies as in **e**.
361 Statistical significance was determined using two-tailed Wilcoxon test. **g,** IC_{50} values for n=30
362 paired neutralizing antibodies isolated at indicated timepoints against indicated mutant SARS-
363 CoV-2 pseudoviruses. Antibodies are divided into groups i-iii, based on neutralizing activity: (i)
364 potent clonal pairs that do not improve over time, (ii) clonal pairs that show increased activity over

365 time, and (iii) and clonal pairs showing decreased neutralization activity after 12 months. Antibody
366 class assignment based on initial (1.3m) sensitivity to mutation is indicated on the right. Red stars
367 indicate antibodies that neutralize all RBD mutants tested. Color gradient indicates IC_{50} values
368 ranging from 0 (white) to 1000 ng/ml (red).

369

370

371 **Methods**

372 **Study participants**.

373 Previously enrolled study participants were asked to return for a 12-month follow-up visit at the
374 Rockefeller University Hospital in New York from February 8 to March 26, 2021. Eligible
375 participants were adults with a history of participation in both prior study visits of our longitudinal
376 cohort study of COVID-19 recovered individuals[3,4]. All participants had a confirmed history of
377 SARS-CoV-2 infection, either diagnosed during the acute infection by RT-PCR or retrospectively
378 confirmed by seroconversion. Exclusion criteria included presence of symptoms suggestive of
379 active SARS-CoV-2 infection. Most study participants were residents of the Greater New York
380 City tri-state region and were asked to return approximately 12 months after the time of onset of
381 COVID-19 symptoms. Participants presented to the Rockefeller University Hospital for blood
382 sample collection and were asked about potential symptom persistence since their 6.2-month study
383 visit, laboratory-confirmed episodes of reinfection with SARS-CoV-2, and whether they had
384 received any COVID-19 related treatment or SARS-CoV-2 vaccination in the interim. Study
385 participants who had received COVID-19 vaccinations, were exclusively recipients of one of the
386 two currently EUA-approved mRNA vaccines, Moderna (mRNA-1273) or Pfizer-BioNTech
387 (BNT162b2), and individuals who received both doses did so according to current interval
388 guidelines, namely 28 days (range 28-30 days) for Moderna and 21 days (range 21-23 days) for
389 Pfizer-BioNtech. Detailed characteristics of the symptomology and severity of the acute infection,
390 symptom kinetics, and the immediate convalescent phase (7 weeks post-symptom onset until
391 6.2month visit) have been reported previously [4]. Participants that presented with persistent
392 symptoms attributable to COVID-19 were identified on the basis of chronic shortness of breath or
393 fatigue, deficit in athletic ability and/or three or more additional long-term symptoms such as

394 persistent unexplained fevers, chest pain, new-onset cardiac sequalae, arthralgias, impairment of
395 concentration/mental acuity, impairment of sense of smell/taste, neuropathy or cutaneous findings
396 as previously described [4]. Clinical data collection and management were carried out using the
397 software iRIS by iMedRIS. All participants at Rockefeller University provided written informed
398 consent before participation in the study and the study was conducted in accordance with Good
399 Clinical Practice. For detailed participant characteristics see Supplementary Table 2. The study
400 was performed in compliance with all relevant ethical regulations and the protocol (DRO-1006)
401 for studies with human participants was approved by the Institutional Review Board of the
402 Rockefeller University.
403
404 **SARS-CoV-2 molecular tests**
405 Saliva was collected into guanidine thiocyanate buffer as described [42]. RNA was extracted using
406 either a column-based (Qiagen QIAmp DSP Viral RNA Mini Kit, Cat#61904) or a magnetic bead-
407 based method as described [43]. Reverse transcribed cDNA was amplified using primers and probes
408 validated by the CDC or by Columbia University Personalized Medicine Genomics Laboratory
409 respectively and approved by the FDA under the Emergency Use Authorization. Viral RNA was
410 considered detected if Ct for two viral primers/probes were <40.
411
412 **Blood samples processing and storage.**
413 Peripheral Blood Mononuclear Cells (PBMCs) obtained from samples collected at Rockefeller
414 University were purified as previously reported by gradient centrifugation and stored in liquid
415 nitrogen in the presence of FCS and DMSO [3,4]. Heparinized plasma and serum samples were

416 aliquoted and stored at -20 °C or less. Prior to experiments, aliquots of plasma samples were
417 heat-inactivated (56 °C for 1 hour) and then stored at 4 °C.
418
419 **ELISAs**
420 ELISAs[44,45] to evaluate antibodies binding to SARS-CoV-2 RBD and N were performed by
421 coating of high-binding 96-half-well plates (Corning 3690) with 50 µl per well of a 1µg/ml
422 protein solution in PBS overnight at 4 °C. Plates were washed 6 times with washing buffer (1×
423 PBS with 0.05% Tween-20 (Sigma-Aldrich)) and incubated with 170 µl per well blocking buffer
424 (1× PBS with 2% BSA and 0.05% Tween-20 (Sigma)) for 1 h at room temperature. Immediately
425 after blocking, monoclonal antibodies or plasma samples were added in PBS and incubated for 1
426 h at room temperature. Plasma samples were assayed at a 1:66 starting dilution and 7 (IgA and
427 IgM anti-RBD) or 11 (IgG anti-RBD) additional threefold serial dilutions. Monoclonal
428 antibodies were tested at 10 µg/ml starting concentration and 10 additional fourfold serial
429 dilutions. Plates were washed 6 times with washing buffer and then incubated with anti-human
430 IgG, IgM or IgA secondary antibody conjugated to horseradish peroxidase (HRP) (Jackson
431 Immuno Research 109-036-088 109-035-129 and Sigma A0295) in blocking buffer at a 1:5,000
432 dilution (IgM and IgG) or 1:3,000 dilution (IgA). Plates were developed by addition of the HRP
433 substrate, TMB (ThermoFisher) for 10 min (plasma samples) or 4 minutes (monoclonal
434 antibodies). The developing reaction was stopped by adding 50 µl 1 M H_2SO_4 and absorbance
435 was measured at 450 nm with an ELISA microplate reader (FluoStar Omega 5.11, BMG
436 Labtech) with Omega MARS software for analysis. For plasma samples, a positive control
437 (plasma from participant COV72, diluted 66.6-fold and seven additional threefold serial dilutions
438 in PBS) was added to every assay plate for validation. The average of its signal was used for

439 normalization of all of the other values on the same plate with Excel software before calculating
440 the area under the curve using Prism V9.1(GraphPad). For monoclonal antibodies, the EC50 was
441 determined using four-parameter nonlinear regression (GraphPad Prism V9.1).
442
443 **Proteins**
444 Mammalian expression vectors encoding the RBDs of SARS-CoV-2 (GenBank MN985325.1; S
445 protein residues 319-539) or K417N, E484K, N501Y RBD mutants with an N-terminal human
446 IL-2 or Mu phosphatase signal peptide were previously described [46]. SARS-CoV-2 nucleocapsid
447 protein (N) was purchased from Sino Biological (40588-V08B).
448
449 **SARS-CoV-2 pseudotyped reporter virus**
450 A panel of plasmids expressing RBD-mutant SARS-CoV-2 spike proteins in the context of
451 pSARS-CoV-2-S $_{\Delta 19}$ has been described previously [2,9,26]. Variant pseudoviruses resembling
452 variants of concern B.1.1.7 (first isolated in the UK), B.1.351 (first isolated in South-Africa),
453 B.1.526 (first isolated in New York City) and P.1 (first isolated in Brazil) were generated by
454 introduction of substitutions using synthetic gene fragments (IDT) or overlap extension PCR
455 mediated mutagenesis and Gibson assembly. Specifically, the variant-specific deletions and
456 substitutions introduced were:
457 B.1.1.7: ΔH69/V70, ΔY144, N501Y, A470D, D614G, P681H, T761I, S982A, D118H
458 B.1.351: D80A, D215G, L242H, R246I, K417N, E484K, N501Y, D614G, A701V
459 B.1.526: L5F, T95I, D253G, E484K, D614G, A701V.
460 P.1: L18F, R20N, P26S, D138Y, R190S, K417T, E484K, N501Y, D614G, H655Y
461

462

463 The E484K and K417N/E484K/N501Y (KEN) substitution, as well as the deletions/substitutions
464 corresponding to variants of concern were incorporated into a spike protein that also includes the
465 R683G substitution, which disrupts the furin cleaveage site and increases particle infectivity.
466 Neutralizing activity against mutant pseudoviruses were compared to a wildtype SARS-CoV-2
467 spike sequence (NC_045512), carrying R683G where appropriate.
468 SARS-CoV-2 pseudotyped particles were generated as previously described [3,13]. Briefly, 293T
469 cells were transfected with pNL4-3ΔEnv-nanoluc and pSARS-CoV-2-$S_{\Delta 19}$, particles were
470 harvested 48 hpt, filtered and stored at -80°C.

471

472 **Microneutralization assay with authentic SARS-CoV-2**.
473 Microneutralization assay of SARS-CoV-2 virus were performed as described previously[3]. The
474 day prior to infection, Vero E6 cells were seeded at $1X10^4$ cells/well into 96-well plates. The
475 diluted plasma and antibodies were mixed with SARS-CoV-2 WA1/2020 or the SA variant
476 B.1.351 and incubated for 1 hour at 37°C. The antibody-virus-mix was then directly applied to
477 Vero E6 cells and incubated for 22 hours at 37°C. Cells were subsequently fixed by adding an
478 equal volume of 70% formaldehyde to the wells, followed by permeabilization with 1% Triton
479 X-100 for 10 minutes. After washing, cells were incubated for 1 hour at 37°C with blocking
480 solution of 5% goat serum in PBS (catalog no. 005–000-121; Jackson ImmunoResearch). A
481 rabbit polyclonal anti-SARS-CoV-2 nucleocapsid antibody (catalog no. GTX135357; GeneTex)
482 was added to the cells at 1:1,000 dilution in blocking solution and incubated at 4 °C overnight.
483 Goat anti-rabbit AlexaFluor 594 (catalog no. A-11012; Life Technologies) was used as a
484 secondary antibody at a dilution of 1:2000. Nuclei were stained with Hoechst 33342 (catalog no.

485 62249; Thermo Fisher Scientific) at 1µg/ml. Images were acquired with a fluorescence
486 microscope and analyzed using ImageXpress Micro XLS (Molecular Devices). All experiments
487 were performed in a biosafety level 3 laboratory.
488
489 **Pseudotyped virus neutralization assay**
490 Fourfold serially diluted plasma from COVID-19-convalescent individuals or monoclonal
491 antibodies were incubated with SARS-CoV-2 pseudotyped virus for 1 h at 37 °C. The mixture
492 was subsequently incubated with $293T_{Ace2}$ cells[3] (for comparisons of plasma or monoclonal
493 antibodies from convalescent individuals) or HT1080Ace2 cl14 cells[13] (for analyses involving
494 mutant/variant pseudovirus panels), as indicated, for 48h after which cells were washed with
495 PBS and lysed with Luciferase Cell Culture Lysis 5× reagent (Promega). Nanoluc Luciferase
496 activity in lysates was measured using the Nano-Glo Luciferase Assay System (Promega) with
497 the Glomax Navigator (Promega). The obtained relative luminescence units were normalized to
498 those derived from cells infected with SARS-CoV-2 pseudotyped virus in the absence of plasma
499 or monoclonal antibodies. The half-maximal neutralization titers for plasma (NT_{50}) or half-
500 maximal and 90% inhibitory concentrations for monoclonal antibodies (IC_{50} and IC_{90}) were
501 determined using four-parameter nonlinear regression (least squares regression method without
502 weighting; constraints: top=1, bottom=0) (GraphPad Prism).
503
504 **Biotinylation of viral protein for use in flow cytometry**
505 Purified and Avi-tagged SARS-CoV-2 RBD or SARS-CoV-2 RBD KEN mutant (K417N,
506 E484K, N501Y) was biotinylated using the Biotin-Protein Ligase-BIRA kit according to
507 manufacturer's instructions (Avidity) as described before [3]. Ovalbumin (Sigma, A5503-1G) was

508 biotinylated using the EZ-Link Sulfo-NHS-LC-Biotinylation kit according to the manufacturer's
509 instructions (Thermo Scientific). Biotinylated ovalbumin was conjugated to streptavidin-BV711
510 (BD biosciences, 563262) and RBD to streptavidin-PE (BD Biosciences, 554061) and
511 streptavidin-AF647 (Biolegend, 405237) [3].
512
513 **Flow cytometry and single cell sorting**
514 Single-cell sorting by flow cytometry was described previously [3]. Briefly, peripheral blood
515 mononuclear cells were enriched for B cells by negative selection using a pan-B-cell isolation kit
516 according to the manufacturer's instructions (Miltenyi Biotec, 130-101-638). The enriched B
517 cells were incubated in FACS buffer (1× PBS, 2% FCS, 1 mM EDTA) with the following anti-
518 human antibodies (all at 1:200 dilution): anti-CD20-PECy7 (BD Biosciences, 335793), anti-
519 CD3-APC-eFluro 780 (Invitrogen, 47-0037-41), anti-CD8-APC-eFluor 780 (Invitrogen, 47-
520 0086-42), anti-CD16-APC-eFluor 780 (Invitrogen, 47-0168-41), anti-CD14-APC-eFluor 780
521 (Invitrogen, 47-0149-42), as well as Zombie NIR (BioLegend, 423105) and fluorophore-labelled
522 RBD and ovalbumin (Ova) for 30 min on ice. Single CD3-CD8-CD14-CD16-CD20+Ova-RBD-
523 PE+RBD-AF647+ B cells were sorted into individual wells of 96-well plates containing 4 µl of
524 lysis buffer (0.5× PBS, 10 mM DTT, 3,000 units/ml RNasin Ribonuclease Inhibitors (Promega,
525 N2615) per well using a FACS Aria III and FACSDiva software (Becton Dickinson) for
526 acquisition and FlowJo for analysis. The sorted cells were frozen on dry ice, and then stored at
527 −80 °C or immediately used for subsequent RNA reverse transcription. For B cell phenotype
528 analysis, in addition to above antibodies, B cells were also stained with following anti-human
529 antibodies: anti- IgG-PECF594 (BD biosciences, 562538), anti-IgM-AF700 (Biolegend,
530 314538), anti-IgA-Viogreen (Miltenyi Biotec, 130-113-481).

531

532 **Antibody sequencing, cloning and expression**

533 Antibodies were identified and sequenced as described previously [3]. In brief, RNA from single
534 cells was reverse-transcribed (SuperScript III Reverse Transcriptase, Invitrogen, 18080-044) and
535 the cDNA stored at −20 °C or used for subsequent amplification of the variable IGH, IGL and
536 IGK genes by nested PCR and Sanger sequencing. Sequence analysis was performed using
537 MacVector. Amplicons from the first PCR reaction were used as templates for sequence- and
538 ligation-independent cloning into antibody expression vectors. Recombinant monoclonal
539 antibodies were produced and purified as previously described [3].

540

541 **Biolayer interferometry**

542 Biolayer interferometry assays were performed as previously described [3]. Briefly, we used the
543 Octet Red instrument (ForteBio) at 30 °C with shaking at 1,000 r.p.m. Epitope-binding assays
544 were performed with protein A biosensor (ForteBio 18-5010), following the manufacturer's
545 protocol 'classical sandwich assay'. (1) Sensor check: sensors immersed 30 s in buffer alone
546 (kinetics buffer 10x ForteBio 18-1105 diluted 1x in PBS1x). (2) Capture first antibody: sensors
547 immersed 10 min with Ab1 at 30 µg/ml. (3) Baseline: sensors immersed 30 s in buffer alone. (4)
548 Blocking: sensors immersed 5 min with IgG isotype control at 50 µg/ml. (6) Antigen association:
549 sensors immersed 5 min with RBD at 100 µg/ml. (7) Baseline: sensors immersed 30 s in buffer
550 alone. (8) Association Ab2: sensors immersed 5 min with Ab2 at 30 µg/ml. Curve fitting was
551 performed using the Fortebio Octet Data analysis software (ForteBio). Affinity measurement of
552 anti-SARS-CoV-2 IgGs binding were corrected by subtracting the signal obtained from traces
553 performed with IgGs in the absence of WT RBD. The kinetic analysis using protein A biosensor

554 (ForteBio 18-5010) was performed as follows: (1) baseline: 60sec immersion in buffer. (2)
555 loading: 200sec immersion in a solution with IgGs 30 μg/ml. (3) baseline: 200sec immersion in
556 buffer. (4) Association: 300sec immersion in solution with WT RBD at 200, 100, 50 or 25 μg/ml
557 (5) dissociation: 600sec immersion in buffer. Curve fitting was performed using a fast 1:1
558 binding model and the Data analysis software (ForteBio). Mean K_D values were determined by
559 averaging all binding curves that matched the theoretical fit with an R^2 value ≥ 0.8.
560

561 **Plasma antibody avidity assay**

562 The plasma SARS-CoV-2 antibody avidity assay were performed as previously described [47].
563

564 **Computational analyses of antibody sequences**

565 Antibody sequences were trimmed based on quality and annotated using Igblastn v.1.14. with
566 IMGT domain delineation system. Annotation was performed systematically using Change-O
567 toolkit v.0.4.540 [48]. Heavy and light chains derived from the same cell were paired, and
568 clonotypes were assigned based on their V and J genes using in-house R and Perl scripts (Fig.
569 2d). All scripts and the data used to process antibody sequences are publicly available on GitHub
570 (https://github.com/stratust/igpipeline).
571

572 The frequency distributions of human V genes in anti-SARS-CoV-2 antibodies from this study
573 was compared to 131,284,220 IgH and IgL sequences generated by [49] and downloaded from
574 cAb-Rep[50], a database of human shared BCR clonotypes available at https://cab-
575 rep.c2b2.columbia.edu/. Based on the 91 distinct V genes that make up the 6902 analyzed
576 sequences from Ig repertoire of the 10 participants present in this study, we selected the IgH and

577 IgL sequences from the database that are partially coded by the same V genes and counted them
578 according to the constant region. The frequencies shown in (Extended data Fig. 4**)** are relative to
579 the source and isotype analyzed. We used the two-sided binomial test to check whether the
580 number of sequences belonging to a specific IgHV or IgLV gene in the repertoire is different
581 according to the frequency of the same IgV gene in the database. Adjusted p-values were
582 calculated using the false discovery rate (FDR) correction. Significant differences are denoted
583 with stars.
584
585 Nucleotide somatic hypermutation and CDR3 length were determined using in-house R and Perl
586 scripts. For somatic hypermutations, IGHV and IGLV nucleotide sequences were aligned against
587 their closest germlines using Igblastn and the number of differences were considered nucleotide
588 mutations. The average mutations for V genes were calculated by dividing the sum of all
589 nucleotide mutations across all participants by the number of sequences used for the analysis.
590
591 Immunoglobulins grouped into the same clonal lineage had their respective IgH and IgL sequences
592 merged and subsequently aligned, using TranslatorX v.1.1 [51], with the unmutated ancestral
593 sequence obtained from IMGT/V-QUEST reference directory [52]. GCTree
594 (https://github.com/matsengrp/gctree) [53] was further used to perform the phylogenetic trees
595 construction. Each node represents a unique IgH and IgL combination and the size of each node is
596 proportional to the number of identical sequences. The numbered nodes represent the unobserved
597 ancestral genotypes between the germline sequence and the sequences on the downstream branch.
598 **Competing interests:** The Rockefeller University has filed a provisional patent application in
599 connection with this work on which M.C.N.is an inventor (US patent 63/021,387). The patent

600 has been licensed by Rockefeller University to Bristol Meyers Squib. Z.Z. received seed
601 instruments and sponsored research funding from ET Healthcare.
602
603 **Data availability statement:** Data are provided in SI Tables 1-8. The raw sequencing data and
604 computer scripts associated with Figure 2 and Extended data figure 5 have been deposited at
605 Github (https://github.com/stratust/igpipeline). This study also uses data from "A Public
606 Database of Memory and Naive B-Cell Receptor Sequences"
607 (https://doi.org/10.5061/dryad.35ks2) and from "High frequency of shared clonotypes in human
608 B cell receptor repertoires" (https://doi.org/10.1038/s41586-019-0934-8).
609
610 **Code availability statement:** Computer code to process the antibody sequences is available at
611 GitHub (https://github.com/stratust/igpipeline).
612
613
614 **Data presentation**
615 Figures arranged in Adobe Illustrator 2020.
616
617 **Acknowledgements:** We thank all study participants who devoted time to our research; The
618 Rockefeller University Hospital nursing staff and Clinical Research Support Office and nursing
619 staff. Mayu Okawa Frank, Marissa Bergh, and Robert B. Darnell for SARS-CoV-2 saliva PCR
620 testing. Pamela J. Bjorkman and all members of the M.C.N. laboratory for helpful discussions and
621 Maša Jankovic for laboratory support. This work was supported by NIH grant P01-AI138398-S1
622 (M.C.N., C.M.R and P.J.B.) and 2U19AI111825 (M.C.N. and C.M.R); George Mason University
623 Fast Grants to C.M.R., 3 R01-AI091707-10S1 to C.M.R.; The G. Harold and Leila Y. Mathers

Charitable Foundation to C.M.R.; NIH grant R37-AI64003 to P.D.B.; NIH grant R01AI78788 to T.H.; We thank Dr. Jost Vielmetter and the Protein Expression Center in the Beckman Institute at Caltech for expression assistance. C.O.B. is supported by the HHMI Hanna Gray and Burroughs Wellcome PDEP fellowships. C.G. was supported by the Robert S. Wennett Post-Doctoral Fellowship, in part by the National Center for Advancing Translational Sciences (National Institutes of Health Clinical and Translational Science Award program, grant UL1 TR001866), and by the Shapiro-Silverberg Fund for the Advancement of Translational Research. P.D.B. and M.C.N. are Howard Hughes Medical Institute Investigators. F.M. is supported by the Bulgari Women & Science Fellowship in COVID-19 Research.

Author Contributions: P.D.B., T.H., C.M.R., and M.C.N. conceived, designed and analyzed the experiments. M. Caskey and C.G. designed clinical protocols. Z.W., F.M., D.S.B., S.F., C.V., H-H.H., C.O.B., A.C., F.S., J.D.S., E.B., L.A., J.Y., M.J. and Z.Z. carried out experiments. A.G. and M. Cipolla produced antibodies. D.S.B., M.D., M.T., K.G.M., C.G. and M. Caskey recruited participants, executed clinical protocols and processed samples. T.Y.O. and V.R. performed bioinformatic analysis. Z.W., F.M., D.S.B., C.G. and M.C.N. wrote the manuscript with input from all co-authors.

Extended Data Figures

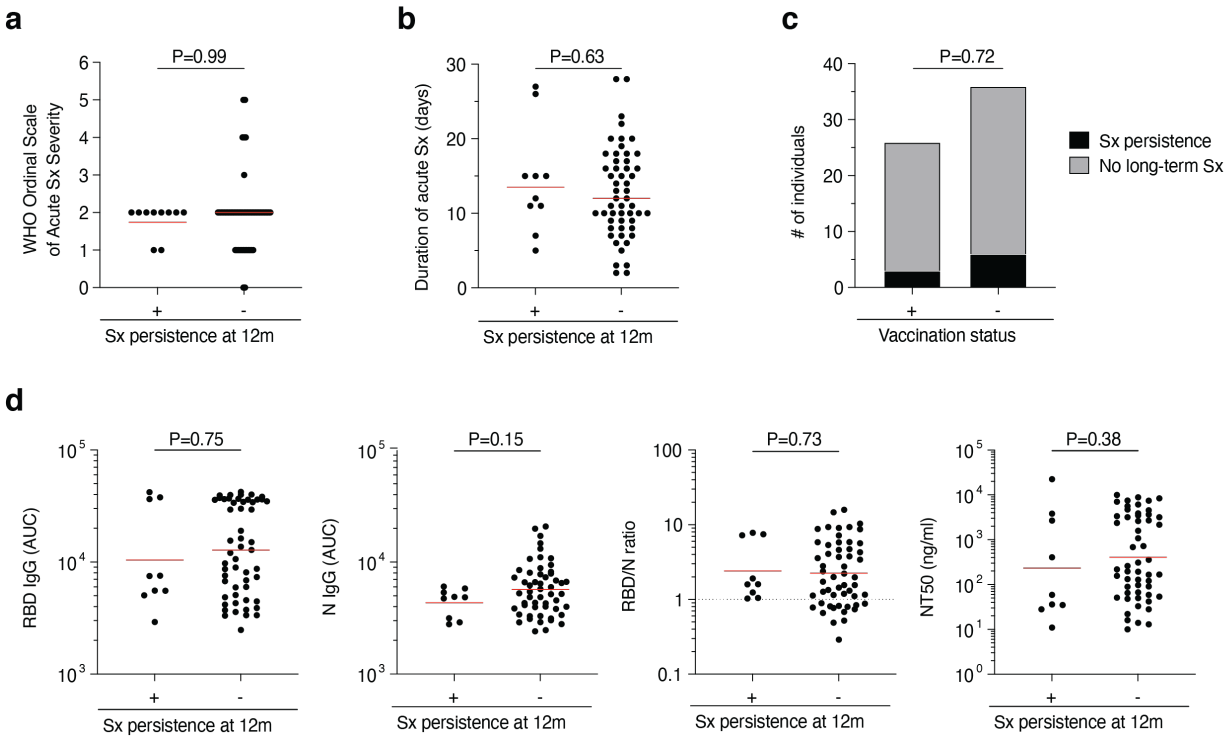

Extended Data Fig. 1 Clinical correlations. a-d, Association of persistence of symptoms (Sx) 12 months after infection with various clinical and serological parameters in our cohort of individuals who recovered from COVID-19 (n=63). **a-b,** Acute disease severity as assessed with the WHO Ordinal Scale of Clinical Improvement (**a**, p=0.99) and duration of acute phase symptoms (**b**, p=0.63) in individuals reporting persistent symptoms (+) compared to individuals who are symptom-free (-) 12 months post-infection. **c,** Proportion of individuals reporting persistent symptoms (black area) compared to individuals who are symptom-free (grey area) 12 months after infection grouped by vaccination status (p=0.72). **d,** Anti-RBD IgG (p=0.75), anti-N IgG (p=0.15), the RBD/N IgG ratio (p=0.73), and NT50 titers (p=0.38) at 12 months after infection in individuals reporting persistent symptoms (+) compared to individuals who are

661 symptom-free (-) 12 months post-infection. Statistical significance was determined using the

662 two-tailed Mann-Whitney test in **a, b** and **d**, and using the two-sided Fisher's exact test in **c**.

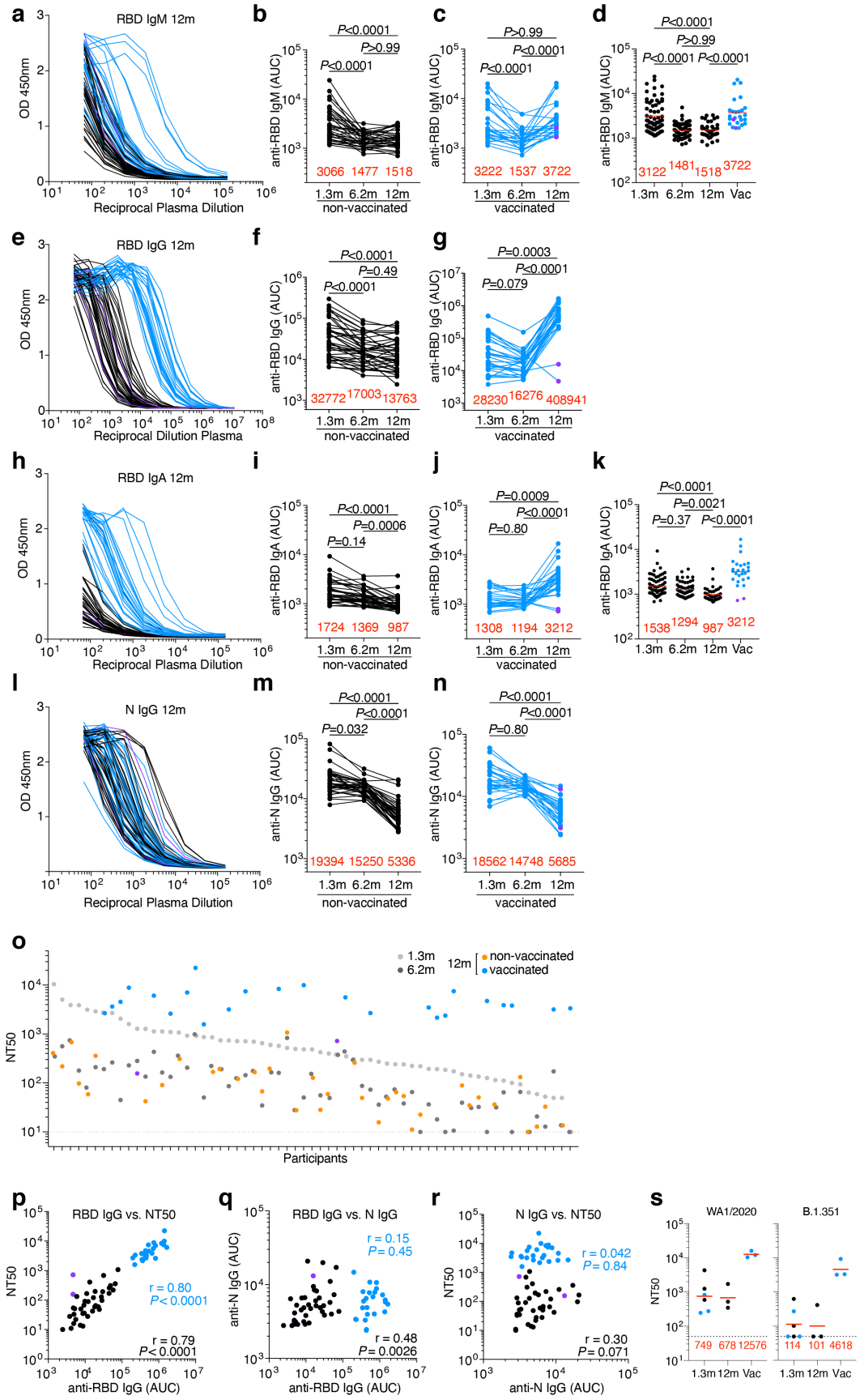
a
RBD IgM 12m
OD 450nm
Reciprocal Plasma Dilution
b
P<0.0001
P>0.99
P<0.0001
anti-RBD IgM (AUC)
3066 1477 1518
1.3m 6.2m 12m
non-vaccinated
c
P>0.99
P<0.0001
P<0.0001
anti-RBD IgM (AUC)
3222 1537 3722
1.3m 6.2m 12m
vaccinated
d
P<0.0001
P>0.99
P<0.0001 P<0.0001
anti-RBD IgM (AUC)
3122 1481 1518 3722
1.3m 6.2m 12m Vac
e
RBD IgG 12m
OD 450nm
Reciprocal Dilution Plasma
f
P<0.0001
P=0.49
P<0.0001
anti-RBD IgG (AUC)
32772 17003 13763
1.3m 6.2m 12m
non-vaccinated
g
P=0.0003
P<0.0001
P=0.079
anti-RBD IgG (AUC)
28230 16276 408941
1.3m 6.2m 12m
vaccinated
h
RBD IgA 12m
OD 450nm
Reciprocal Plasma Dilution
i
P<0.0001
P=0.0006
P=0.14
anti-RBD IgA (AUC)
1724 1369 987
1.3m 6.2m 12m
non-vaccinated
j
P=0.0009
P<0.0001
P=0.80
anti-RBD IgA (AUC)
1308 1194 3212
1.3m 6.2m 12m
vaccinated
k
P<0.0001
P=0.0021
P=0.37 P<0.0001
anti-RBD IgA (AUC)
1538 1294 987 3212
1.3m 6.2m 12m Vac
l
N IgG 12m
OD 450nm
Reciprocal Plasma Dilution
m
P<0.0001
P<0.0001
P=0.032
anti-N IgG (AUC)
19394 15250 5336
1.3m 6.2m 12m
non-vaccinated
n
P<0.0001
P<0.0001
P=0.80
anti-N IgG (AUC)
18562 14748 5685
1.3m 6.2m 12m
vaccinated
o
1.3m
6.2m
12m
non-vaccinated
vaccinated
NT50
Participants
p
RBD IgG vs. NT50
NT50
r = 0.80
P< 0.0001
r = 0.79
P< 0.0001
anti-RBD IgG (AUC)
q
RBD IgG vs. N IgG
anti-N IgG (AUC)
r = 0.15
P= 0.45
r = 0.48
P= 0.0026
anti-RBD IgG (AUC)
r
N IgG vs. NT50
NT50
r = 0.042
P= 0.84
r = 0.30
P= 0.071
anti-N IgG (AUC)
s
WA1/2020
B.1.351
NT50
749 678 12576
114 101 4618
1.3m 12m Vac
1.3m 12m Vac

663

664 **Extended Data Fig. 2: Plasma activity. a-h,** ELISA results for plasma against SARS-CoV-2
665 RBD 12 months after infection (n=63). Non-vaccinated individuals are depicted with black circles
666 and lines, and vaccinated individuals are depicted in blue throughout. Two outlier individuals who
667 received their first dose of vaccine 24-48 hours before sample collection is depicted as purple
668 circles. **a-n,** IgM (**a-d**) IgG (**e-g**) and IgA (**h-k**) antibody binding to SARS-CoV-2 RBD and IgG
669 binding to N (**l-n**) 12 months after infection. **a, e, h, I,** ELISA curves from non-vaccinated (black
670 lines) individuals, as well as individuals who received one or two doses (blue lines) of a COVID-
671 19 mRNA vaccine (left panels). Area under the curve (AUC) over time in non-vaccinated (**b, f, i**
672 and **m**) and vaccinated individuals (**c, g, j,** and **n**). Lines connect longitudinal samples. **d, k,**
673 Boxplots showing AUC values of all 63 individuals, as indicated. **o,** ranked average NT50 at 1.3
674 months (light grey) and 6.2 months (dark grey), as well as at 12 months for non-vaccinated
675 (orange) individuals, and individuals who received one or two doses (blue circles) of a COVID-
676 19 mRNA vaccine, respectively. Two individuals who received their first dose of vaccine 24-48
677 hours before sample collection is depicted in purple. **p-r,** Correlation of serological parameters in
678 non-vaccinated (black circles and black statistics) and vaccinated (blue circles and blue statistics)
679 individuals. Two individuals who received their first dose of vaccine 24-48 hours before sample
680 collection is depicted as purple circles. Correlation of 12-month titers of anti- RBD IgG and NT50
681 (**p**), anti-RBD IgG and N IgG (**q**), and anti-N IgG and NT50 (**r**). **s,** Plasma neutralizing activity
682 against authentic virus isolates WA1/2020 and B.1.351, as indicated (n=6). Statistical significance
683 was determined using two-sided Friedman test with subsequent Dunn's multiple comparisons
684 (**b**,**c**,**f**,**g**,**i**,**j**,**m**,**n**), or two-sided Kruskal-Wallis test with subsequent Dunn's multiple comparisons
685 (**d** and **k**) or using the Spearman correlation test for the non-vaccinated and vaccinated subgroups
686 independently (**p-r**) or using two-tailed Mann-Whitney test (**s**). Red numbers indicate the

687 geometric mean NT50 at the indicated timepoint. All experiments were performed at least in
688 duplicate.

689

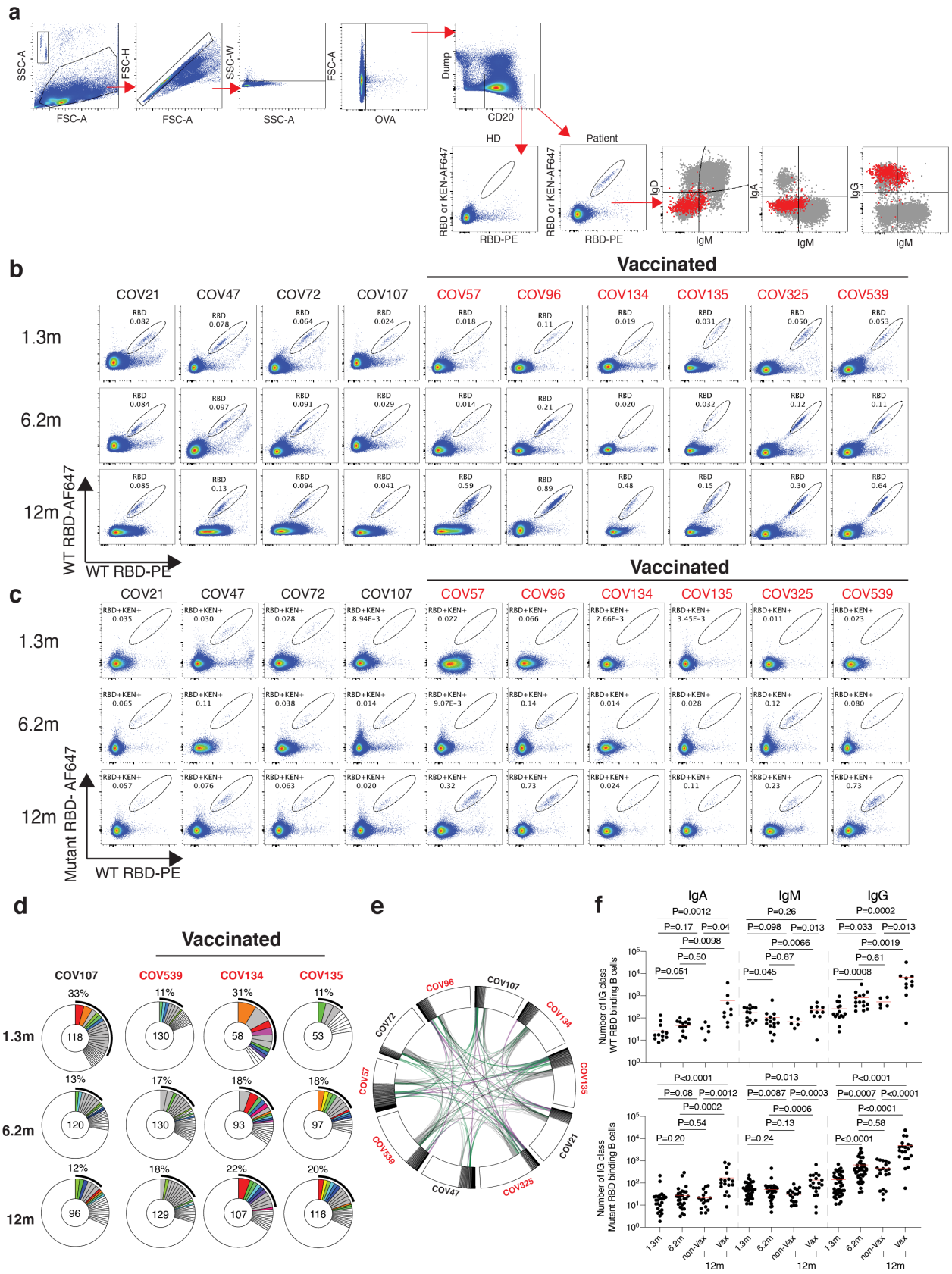
a
SSC-A
FSC-A
FSC-H
FSC-A
SSC-W
SSC-A
FSC-A
OVA
Dump
CD20
HD
Patient
RBD or KEN-AF647
RBD-PE
IgD
IgM
IgA
IgG
b
Vaccinated
COV21
COV47
COV72
COV107
COV57
COV96
COV134
COV135
COV325
COV539
1.3m
6.2m
12m
WT RBD-AF647
WT RBD-PE
c
Mutant RBD- AF647
d
e
f
IgA
IgM
IgG
Number of IG class WT RBD binding B cells
Number of IG class Mutant RBD binding B cells
1.3m
6.2m
non-Vax
Vax
12m

691 **Extended Data Fig. 3: Flow cytometry. a,** Gating strategy. Gating was on singlets that were
692 $CD20^+$ and CD3-CD8-CD16-Ova-. Anti-IgG, IgM, and IgA antibodies were used for B cell
693 phenotype analysis. Sorted cells were RBD-PE^+ and RBD/KEN-$AF647^+$. **b and c,** Flow cytometry
694 showing the percentage of RBD-double positive (**b**) and 647-K417N/E484K/N501Y mutant RBD
695 cross-reactive (**c**) memory B cells from 1.3 or 6- and 12-months post-infection in 10 selected
696 participants. **d**. as in Fig. 2b, Pie charts show the distribution of antibody sequences from 4
697 individuals after 1.3 [3] (upper panel) or 6.2[4] months (middle panel) or 12 months (lower panel). **e,**
698 Circos plot depicts the relationship between antibodies that share V and J gene segment sequences
699 at both IGH and IGL. Purple, green, and grey lines connect related clones, clones and singles, and
700 singles to each other, respectively. **f,** graph summarizes cell number (indicated in **b** and **c**) (per 2
701 million B cells) of immunoglobulin class of antigens binding memory B cells in samples obtained
702 at 1.3, 6.2 and 12 months. Each dot is one individual. (Vaccinees, n=20, and non-vaccinees, n=20).
703 Red horizontal bars indicate mean values. Statistical significance was determined using two-sided
704 Kruskal-Wallis test with subsequent Dunn's multiple comparisons.
705

706

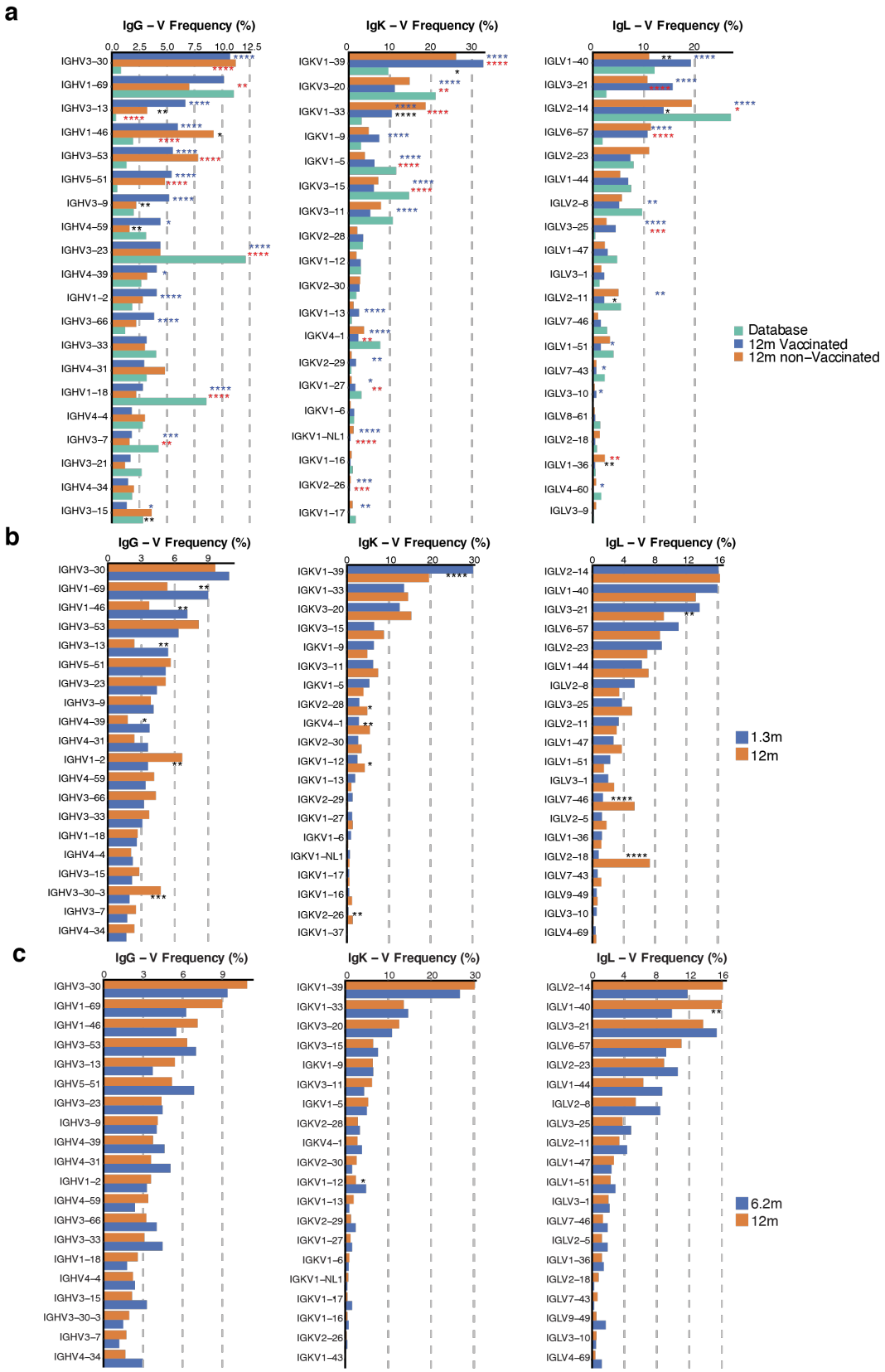
a
IgG – V Frequency (%)
IgK – V Frequency (%)
IgL – V Frequency (%)
Database
12m Vaccinated
12m non–Vaccinated
b
IgG – V Frequency (%)
IgK – V Frequency (%)
IgL – V Frequency (%)
1.3m
12m
c
IgG – V Frequency (%)
IgK – V Frequency (%)
IgL – V Frequency (%)
6.2m
12m

707

708 **Extended Data Fig. 4: Frequency distribution of human V genes.** Graph shows comparison of
709 the frequency distributions of human V genes of anti-SARS-CoV-2 antibodies from donors at 1.3[3],
710 6.2[4], 12 months after infection. **a,** Graph shows relative abundance of human IGVH genes
711 Sequence Read Archive accession SRP010970 (green), convalescent vaccinees (blue), and
712 convalescent non-vaccinees (orange). Statistical significance was determined by two-sided
713 binomial test. **b and c,** same as in **a**, but showing comparison between antibodies from donors at
714 1.3 months[3] (**b**), 6.2 month[4] (**c**), and 12 months after infection. Two-sided binomial tests with
715 unequal variance were used to compare the frequency distributions., significant differences are
716 denoted with stars (* $p < 0.05$, ** $p < 0.01$, *** $p < 0.001$, **** = $p < 0.0001$).
717

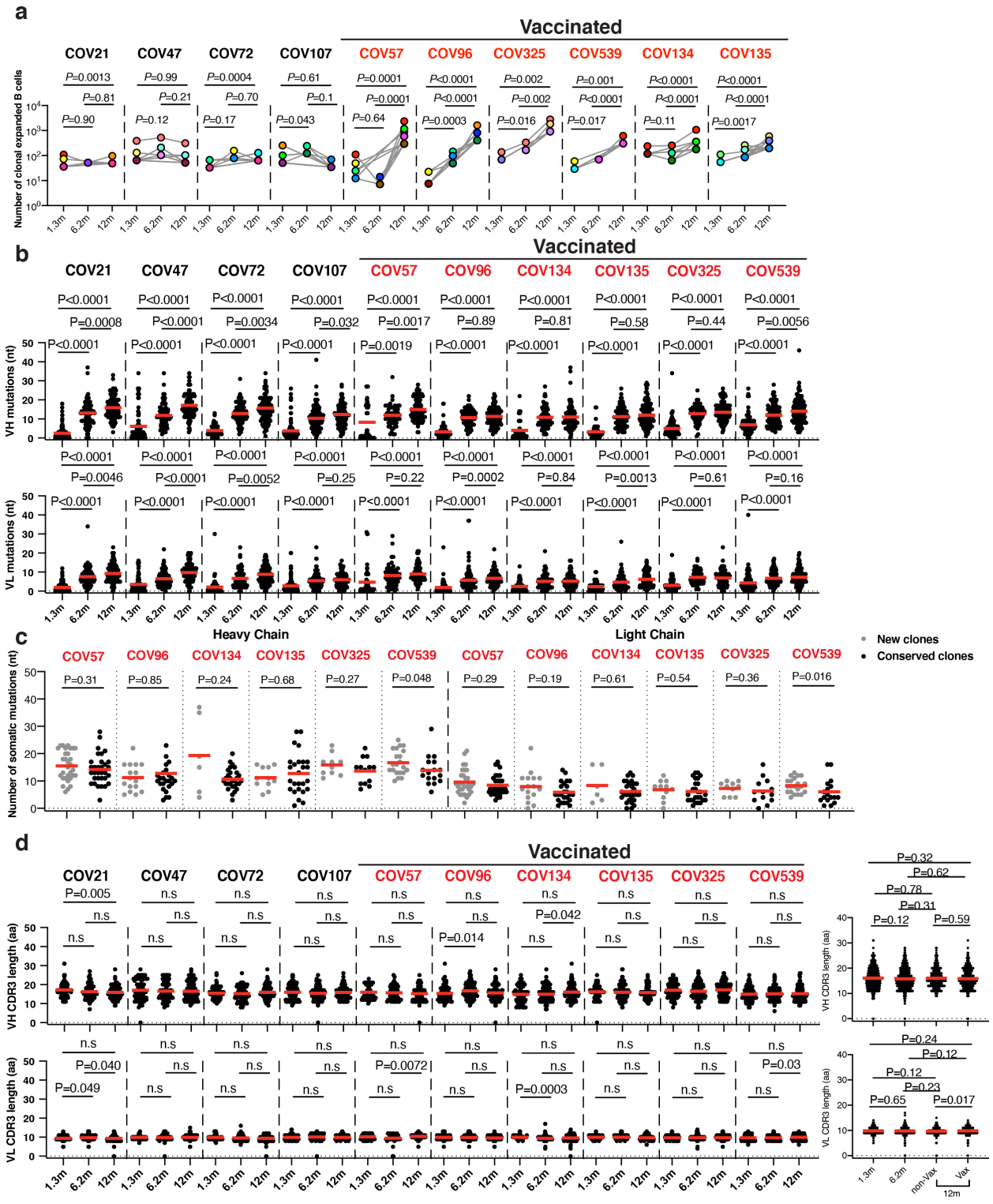
a
Vaccinated
COV21
COV47
COV72
COV107
COV57
COV96
COV325
COV539
COV134
COV135
Number of clonal expanded B cells
b
VH mutations (nt)
VL mutations (nt)
Heavy Chain
Light Chain
c
Number of somatic mutations (nt)
New clones
Conserved clones
d
VH CDR3 length (aa)
VL CDR3 length (aa)
non-Vax
Vax
12m

718

719

720 **Extended Data Fig. 5: Analysis of anti-RBD antibodies. a**, Number of clonally expanded B cells
721 (per 10 million B cells) at indicated time points in 10 individuals. Colors indicate shared clones
722 appearing at different time points. Statistical significance was determined using two-tailed
723 Wilcoxon matched-pairs signed rank test. Vaccinees are marked in red. Statistical significance was
724 determined using Wilcoxon matched-pairs signed rank tests. Vaccinees are marked in red. **b.**
725 Number of somatic nucleotide mutations in the IGVH (top) and IGVL (bottom) in antibodies
726 obtained after 1.3 or 6.2 or 12 months from the indicated individual. **c.** same as **b**, but graphs show
727 comparison between new clones and conserved clones in 6 vaccinated convalescent individuals at
728 12 months after infection. **d.** The amino acid length of the CDR3s at the IGVH and IGVL for each
729 individual. Right panel shows all antibodies combined. (1.3m: n=889; 6.2m: n=975; 12m: n=1105,
730 (non-vax: n=417; vax: n=688)). The horizontal bars indicate the mean. Statistical significance was
731 determined using two-sided Kruskal-Wallis test with subsequent Dunn's multiple comparisons (**a,**
732 **b** and **d**), or two-tailed Mann–Whitney U-tests (**c**).
733

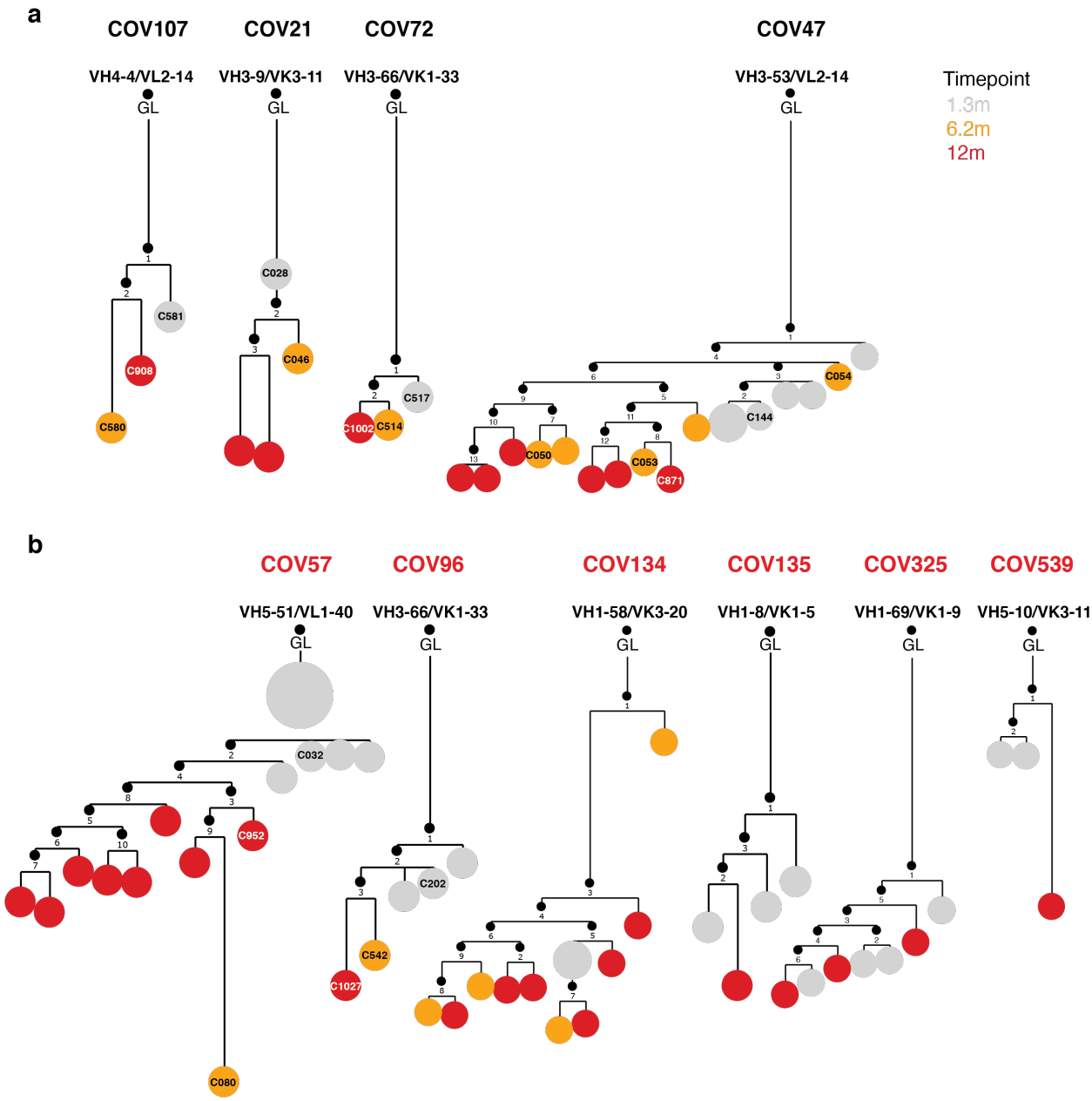

Extended Data Fig. 6: Evolution of anti-SARS-CoV-2 RBD antibody clone. Clonal evolution of RBD-binding memory B cells from ten convalescent individuals, **a**, phylogenetic tree graph shows clones from convalescent non-vaccinees, **b**, same as **a**, but from convalescent vaccinees. Numbers refer to mutations compared to the preceding vertical node. Colors indicate timepoint;

740 grey, orange and red represent 1.3, 6 and 12 months respectively, black dots indicate inferred

741 nodes, and size is proportional to sequence copy number; GL = germline sequence.

742

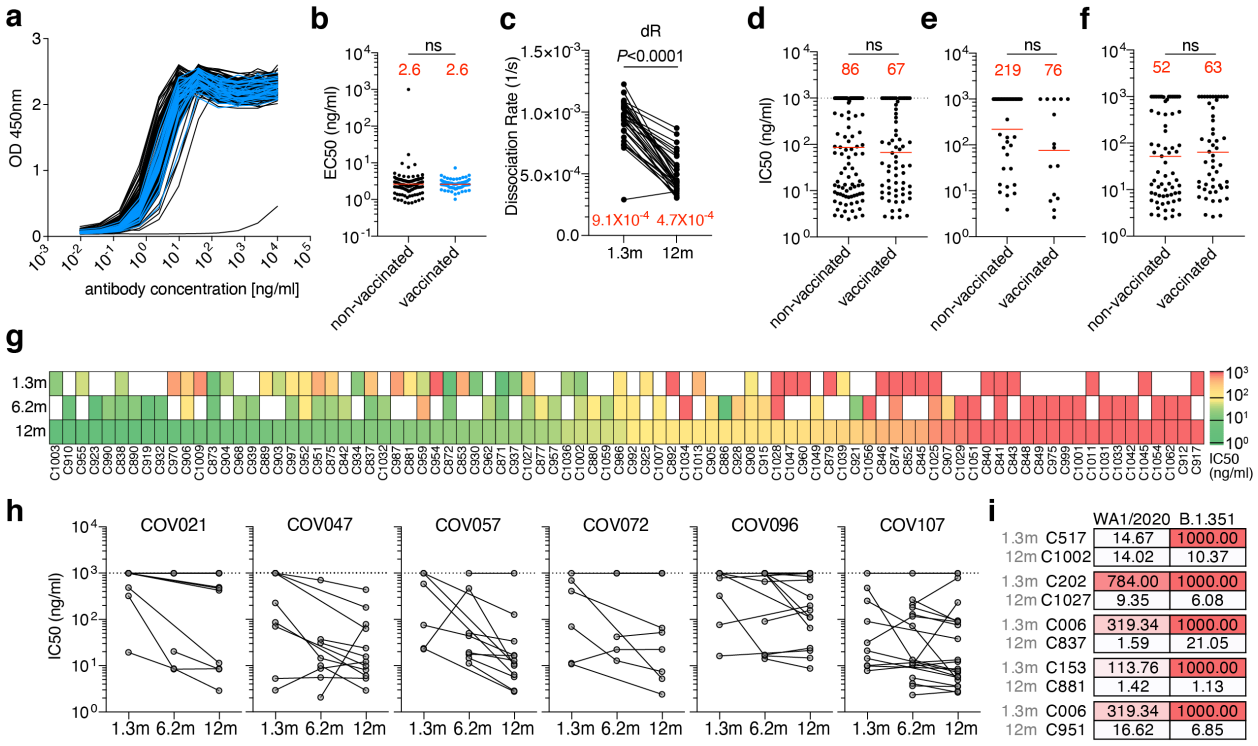

Extended Data Fig. 7: WT RBD binding and pseudovirus neutralization. a,b, Binding curves (**a**) and EC_{50} dot plot (**b**) of mAbs isolated from non-vaccinated (black curves and dots) and from vaccinated (blue curves and dots) convalescents individuals 12 months after infection (p=0.74). **c,** Avidity (dissociation rate) measuring plasma reactivity to RBD at the 1.3- and 12-month follow-up visit (n=33). **d-f,** IC_{50} values of mAbs isolated 12 months after infection from non-vaccinated and vaccinated individuals. **d** shows all 12-month antibodies irrespective of clonality, **e** shows singlets only, and **f** shows only antibodies belonging to a clone or shared over time. Statistical significance in **b, d-f** was determined using the two-tailed Mann-Whitney test; **c** was determined using two-tailed Wilcoxon test. The geometric mean EC_{50} and IC_{50} are indicated in red. **g.** Heat map shows the neutralizing activity of clonally related antibodies against wt-SARS-CoV-2 over time. White tiles indicate no clonal relative at the respective time point. Clones are ranked from left to right by the potency of the 12-month progeny antibodies which are denoted below the tiles.

756 **h,** IC_{50} values of shared clones of mAbs cloned from B cells from the initial 1.3- and 6.2, as well
757 as 12-month follow-up visit, divided by participant, as indicated. Lines connect clonal antibodies
758 shared between time points. Antibodies with IC50>1000ng/ml are plotted at 1000 ng/ml in panels
759 d-h. **i**, IC_{50} values of 5 neutralizing antibody pairs against indicated authentic SARS-CoV-2
760 WA1/2020 and B.1.351 viruses (n=10). Average EC_{50} and IC_{50} values of two independent
761 experiments are shown.
762
763

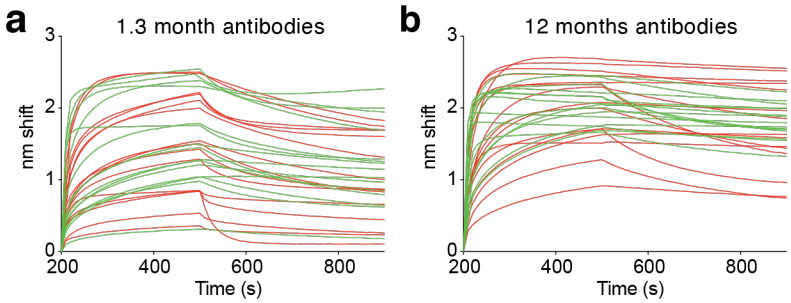

Extended Data Fig. 8: Biolayer interferometry affinity measurements. a-b, Graphs depict affinity measurements of neutralizing (green) and non-neutralizing (red) antibodies isolated 1.3 months (**a)** or 12 months (**b)** after infection.

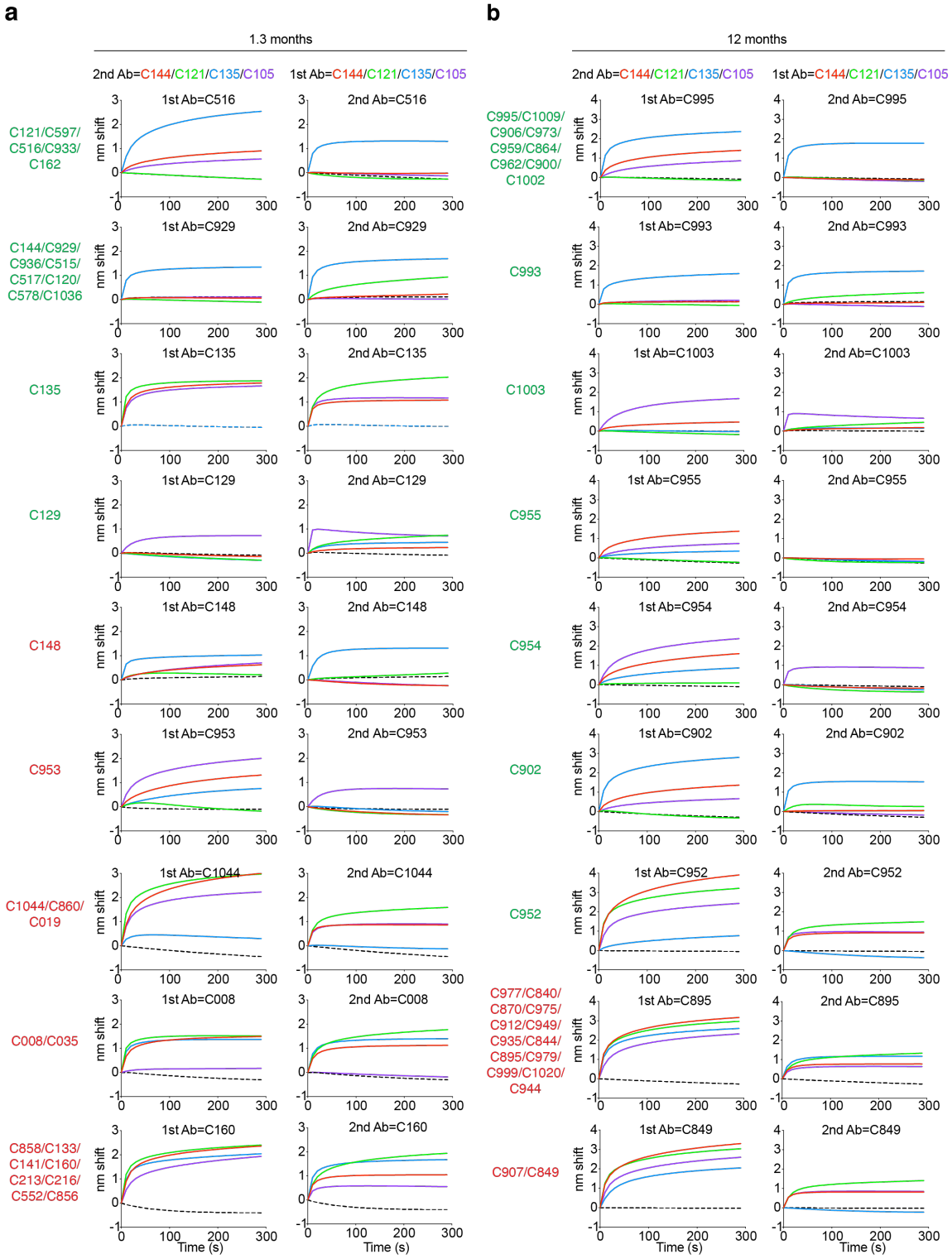
a
1.3 months
2nd Ab=C144/C121/C135/C105
1st Ab=C144/C121/C135/C105
C121/C597/C516/C933/C162
1st Ab=C516
2nd Ab=C516
C144/C929/C936/C515/C517/C120/C578/C1036
1st Ab=C929
2nd Ab=C929
C135
1st Ab=C135
2nd Ab=C135
C129
1st Ab=C129
2nd Ab=C129
C148
1st Ab=C148
2nd Ab=C148
C953
1st Ab=C953
2nd Ab=C953
C1044/C860/C019
1st Ab=C1044
2nd Ab=C1044
C008/C035
1st Ab=C008
2nd Ab=C008
C858/C133/C141/C160/C213/C216/C552/C856
1st Ab=C160
2nd Ab=C160
nm shift
Time (s)
b
12 months
2nd Ab=C144/C121/C135/C105
1st Ab=C144/C121/C135/C105
C995/C1009/C906/C973/C959/C864/C962/C900/C1002
1st Ab=C995
2nd Ab=C995
C993
1st Ab=C993
2nd Ab=C993
C1003
1st Ab=C1003
2nd Ab=C1003
C955
1st Ab=C955
2nd Ab=C955
C954
1st Ab=C954
2nd Ab=C954
C902
1st Ab=C902
2nd Ab=C902
C952
1st Ab=C952
2nd Ab=C952
C977/C840/C870/C975/C912/C949/C935/C844/C895/C979/C999/C1020/C944
1st Ab=C895
2nd Ab=C895
C907/C849
1st Ab=C849
2nd Ab=C849
nm shift
Time (s)

772 **Extended Data Fig. 9: Biolayer interferometry antibody competition experiment. a-b,** Anti-
773 SARS-CoV-2 RBD antibodies isolated 1.3 (**a**) or 12 months (**b**) after infection were assayed for
774 competition with structurally characterized anti-RBD antibodies by biolayer interferometry
775 experiments as in Fig 4a. Graphs represent the binding of the second antibody (2nd Ab) to
776 preformed first antibody (1st Ab)–RBD complexes. Dotted line denotes when 1st Ab and 2nd Ab
777 are the same. For each antibody group identified in Fig 4c the left graphs represent the binding of
778 the class-representative C144, C121, C135 or C105 [3,23](2nd Ab) to the candidate antibody (1st
779 Ab)-RBD complex. The right graphs represent the binding of the candidate antibody (2nd Ab) to
780 the complex of C144-RBD, C121-RBD, C135-RBD or C105-RBD (1st Ab). Antibodies belonging
781 to the same groups are indicated to the left of the respective curves.
782

783 ## Supplementary Tables

784 **Supplementary Table 1: Cohort summary**

785 **Supplementary Table 2: Individual participant characteristics**

786 **Supplementary Table 3: Antibody sequences from patients is provided as a separate Excel**
787 **file.**

788 **Supplementary Table 4: Sequences, half maximal effective concentrations (EC50s) and**
789 **inhibitory concentrations (IC50s) of the cloned monoclonal antibodies is provided as a**
790 **separate Excel file.**

791 **Supplementary Table 5: Binding and Neutralization activity of mAbs against mutant**
792 **SARS-CoV-2 pseudoviruses.**

793 **Supplementary Table 6: Neutralization activity of mAbs against mutant SARS-CoV-2**
794 **pseudoviruses - Random potently neutralizing antibodies isolated at 1.3 and 12 months**

795 **Supplementary Table 7: Antibody affinities and neutralization - Clonal pairs isolated at 1.3**
796 **and 12 months**

797 **Supplementary Table 8: Neutralization activity of mAbs against mutant SARS-CoV-2**
798 **pseudoviruses - Clonal pairs isolated at 1.3 and 12 months.**

799

800 **Reference:**

801 1 Davies, N. G. *et al.* Estimated transmissibility and impact of SARS-CoV-2 lineage B.1.1.7
802 in England. *Science* **372**, doi:10.1126/science.abg3055 (2021).
803 2 Wang, Z. *et al.* mRNA vaccine-elicited antibodies to SARS-CoV-2 and circulating variants.
804 *Nature* **592**, 616-622, doi:10.1038/s41586-021-03324-6 (2021).
805 3 Robbiani, D. F. *et al.* Convergent antibody responses to SARS-CoV-2 in convalescent
806 individuals. *Nature* **584**, 437-442, doi:10.1038/s41586-020-2456-9 (2020).
807 4 Gaebler, C. *et al.* Evolution of antibody immunity to SARS-CoV-2. *Nature* **591**, 639-644,
808 doi:10.1038/s41586-021-03207-w (2021).
809 5 Goel, R. R. *et al.* Distinct antibody and memory B cell responses in SARS-CoV-2 naive and
810 recovered individuals following mRNA vaccination. *Sci Immunol* **6**,
811 doi:10.1126/sciimmunol.abi6950 (2021).
812 6 Saadat, S. *et al.* Binding and Neutralization Antibody Titers After a Single Vaccine Dose in
813 Health Care Workers Previously Infected With SARS-CoV-2. *JAMA* **325**, 1467-1469,
814 doi:10.1001/jama.2021.3341 (2021).
815 7 Krammer, F. *et al.* Antibody Responses in Seropositive Persons after a Single Dose of
816 SARS-CoV-2 mRNA Vaccine. *N Engl J Med* **384**, 1372-1374, doi:10.1056/NEJMc2101667
817 (2021).
818 8 Reynolds, C. J. *et al.* Prior SARS-CoV-2 infection rescues B and T cell responses to
819 variants after first vaccine dose. *Science*, doi:10.1126/science.abh1282 (2021).
820 9 Muecksch, F. *et al.* Development of potency, breadth and resilience to viral escape
821 mutations in SARS-CoV-2 neutralizing antibodies. *bioRxiv*,
822 doi:10.1101/2021.03.07.434227 (2021).
823 10 Brouwer, P. J. M. *et al.* Potent neutralizing antibodies from COVID-19 patients define
824 multiple targets of vulnerability. *Science* **369**, 643-650, doi:10.1126/science.abc5902
825 (2020).
826 11 Cao, Y. *et al.* Potent Neutralizing Antibodies against SARS-CoV-2 Identified by High-
827 Throughput Single-Cell Sequencing of Convalescent Patients' B Cells. *Cell* **182**, 73-84 e16,
828 doi:10.1016/j.cell.2020.05.025 (2020).
829 12 Ju, B. *et al.* Human neutralizing antibodies elicited by SARS-CoV-2 infection. *Nature* **584**,
830 115-119, doi:10.1038/s41586-020-2380-z (2020).
831 13 Schmidt, F. *et al.* Measuring SARS-CoV-2 neutralizing antibody activity using
832 pseudotyped and chimeric viruses. *J Exp Med* **217**, doi:10.1084/jem.20201181 (2020).
833 14 Tegally, H. *et al.* Detection of a SARS-CoV-2 variant of concern in South Africa. *Nature*
834 **592**, 438-443, doi:10.1038/s41586-021-03402-9 (2021).
835 15 West, A. P. *et al.* Detection and characterization of the SARS-CoV-2 lineage B.1.526 in
836 New York. *bioRxiv*, 2021.2002.2014.431043, doi:10.1101/2021.02.14.431043 (2021).
837 16 Inoue, T. *et al.* Exit from germinal center to become quiescent memory B cells depends
838 on metabolic reprograming and provision of a survival signal. *J Exp Med* **218**,
839 doi:10.1084/jem.20200866 (2021).
840 17 Viant, C. *et al.* Antibody Affinity Shapes the Choice between Memory and Germinal
841 Center B Cell Fates. *Cell* **183**, 1298-1311 e1211, doi:10.1016/j.cell.2020.09.063 (2020).

842 18 Rogers, T. F. *et al.* Isolation of potent SARS-CoV-2 neutralizing antibodies and protection
843 from disease in a small animal model. *Science* **369**, 956-963,
844 doi:10.1126/science.abc7520 (2020).
845 19 Kreer, C. *et al.* Longitudinal Isolation of Potent Near-Germline SARS-CoV-2-Neutralizing
846 Antibodies from COVID-19 Patients. *Cell* **182**, 1663-1673, doi:10.1016/j.cell.2020.08.046
847 (2020).
848 20 Stamatatos, L. *et al.* mRNA vaccination boosts cross-variant neutralizing antibodies
849 elicited by SARS-CoV-2 infection. *Science*, doi:10.1126/science.abg9175 (2021).
850 21 Sokal, A. *et al.* Maturation and persistence of the anti-SARS-CoV-2 memory B cell
851 response. *Cell* **184**, 1201-1213 e1214, doi:10.1016/j.cell.2021.01.050 (2021).
852 22 Sakharkar, M. *et al.* Prolonged evolution of the human B cell response to SARS-CoV-2
853 infection. *Sci Immunol* **6**, doi:10.1126/sciimmunol.abg6916 (2021).
854 23 Barnes, C. O. *et al.* SARS-CoV-2 neutralizing antibody structures inform therapeutic
855 strategies. *Nature* **588**, 682-687, doi:10.1038/s41586-020-2852-1 (2020).
856 24 Hoffmann, M. *et al.* SARS-CoV-2 Cell Entry Depends on ACE2 and TMPRSS2 and Is
857 Blocked by a Clinically Proven Protease Inhibitor. *Cell* **181**, 271-280 e278,
858 doi:10.1016/j.cell.2020.02.052 (2020).
859 25 Greaney, A. J. *et al.* Mutational escape from the polyclonal antibody response to SARS-
860 CoV-2 infection is largely shaped by a single class of antibodies. *bioRxiv*,
861 doi:10.1101/2021.03.17.435863 (2021).
862 26 Weisblum, Y. *et al.* Escape from neutralizing antibodies by SARS-CoV-2 spike protein
863 variants. *Elife* **9**, doi:10.7554/eLife.61312 (2020).
864 27 Elsner, R. A. & Shlomchik, M. J. Germinal Center and Extrafollicular B Cell Responses in
865 Vaccination, Immunity, and Autoimmunity. *Immunity* **53**, 1136-1150,
866 doi:10.1016/j.immuni.2020.11.006 (2020).
867 28 Lau, A. W. & Brink, R. Selection in the germinal center. *Curr Opin Immunol* **63**, 29-34,
868 doi:10.1016/j.coi.2019.11.001 (2020).
869 29 Victora, G. D. & Nussenzweig, M. C. Germinal centers. *Annu Rev Immunol* **30**, 429-457,
870 doi:10.1146/annurev-immunol-020711-075032 (2012).
871 30 Inoue, T., Moran, I., Shinnakasu, R., Phan, T. G. & Kurosaki, T. Generation of memory B
872 cells and their reactivation. *Immunol Rev* **283**, 138-149, doi:10.1111/imr.12640 (2018).
873 31 Taylor, J. J., Pape, K. A., Steach, H. R. & Jenkins, M. K. Humoral immunity. Apoptosis and
874 antigen affinity limit effector cell differentiation of a single naive B cell. *Science* **347**,
875 784-787, doi:10.1126/science.aaa1342 (2015).
876 32 McKean, D. *et al.* Generation of antibody diversity in the immune response of BALB/c
877 mice to influenza virus hemagglutinin. *Proc Natl Acad Sci U S A* **81**, 3180-3184,
878 doi:10.1073/pnas.81.10.3180 (1984).
879 33 Petersen, M. S. *et al.* SARS-CoV-2 natural antibody response persists up to 12 months in
880 a nationwide study from the Faroe Islands. *medRxiv*, 2021.2004.2019.21255720,
881 doi:10.1101/2021.04.19.21255720 (2021).
882 34 Li, C. *et al.* Twelve-month specific IgG response to SARS-CoV-2 receptor-binding domain
883 among COVID-19 convalescent plasma donors in Wuhan. *bioRxiv*,
884 2021.2004.2005.437224, doi:10.1101/2021.04.05.437224 (2021).

885 35 Turner, J. *et al.* SARS-CoV-2 mRNA vaccines induce a robust germinal centre reaction in
886 humans. *Research Square*, doi:https://www.researchsquare.com/article/rs-310773/v1
887 (2021).
888 36 Greaney, A. J. *et al.* The SARS-CoV-2 mRNA-1273 vaccine elicits more RBD-focused
889 neutralization, but with broader antibody binding within the RBD. *bioRxiv*,
890 doi:10.1101/2021.04.14.439844 (2021).
891 37 Wang, Z. *et al.* Enhanced SARS-CoV-2 neutralization by dimeric IgA. *Sci Transl Med* **13**,
892 doi:10.1126/scitranslmed.abf1555 (2021).
893 38 Schoof, M. *et al.* An ultrapotent synthetic nanobody neutralizes SARS-CoV-2 by
894 stabilizing inactive Spike. *Science* **370**, 1473-1479, doi:10.1126/science.abe3255 (2020).
895 39 De Gasparo, R. *et al.* Bispecific IgG neutralizes SARS-CoV-2 variants and prevents escape
896 in mice. *Nature*, doi:10.1038/s41586-021-03461-y (2021).
897 40 Xu, J. *et al.* Multimeric nanobodies from camelid engineered mice and llamas potently
898 neutralize SARS-CoV-2 variants. *bioRxiv*, doi:10.1101/2021.03.04.433768 (2021).
899 41 Wu, F. *et al.* A new coronavirus associated with human respiratory disease in China.
900 *Nature* **579**, 265-269, doi:10.1038/s41586-020-2008-3 (2020).
901 42 Chomczynski, P. & Sacchi, N. Single-step method of RNA isolation by acid guanidinium
902 thiocyanate-phenol-chloroform extraction. *Analytical biochemistry* **162**, 156-159,
903 doi:10.1006/abio.1987.9999 (1987).
904 43 DeAngelis, M. M., Wang, D. G. & Hawkins, T. L. Solid-phase reversible immobilization for
905 the isolation of PCR products. *Nucleic Acids Res* **23**, 4742-4743,
906 doi:10.1093/nar/23.22.4742 (1995).
907 44 Grifoni, A. *et al.* Targets of T Cell Responses to SARS-CoV-2 Coronavirus in Humans with
908 COVID-19 Disease and Unexposed Individuals. *Cell* **181**, 1489-1501 e1415,
909 doi:10.1016/j.cell.2020.05.015 (2020).
910 45 Amanat, F. *et al.* A serological assay to detect SARS-CoV-2 seroconversion in humans.
911 *Nat Med* **26**, 1033-1036, doi:10.1038/s41591-020-0913-5 (2020).
912 46 Barnes, C. O. *et al.* Structures of Human Antibodies Bound to SARS-CoV-2 Spike Reveal
913 Common Epitopes and Recurrent Features of Antibodies. *Cell* **182**, 828-842 e816,
914 doi:10.1016/j.cell.2020.06.025 (2020).
915 47 Racine-Brzostek, S. E. *et al.* TOP-Plus is a Versatile Biosensor Platform for Monitoring
916 SARS-CoV-2 Antibody Durability. *Clin Chem*, doi:10.1093/clinchem/hvab069 (2021).
917 48 Gupta, N. T. *et al.* Change-O: a toolkit for analyzing large-scale B cell immunoglobulin
918 repertoire sequencing data. *Bioinformatics (Oxford, England)* **31**, 3356-3358,
919 doi:10.1093/bioinformatics/btv359 (2015).
920 49 Soto, C. *et al.* High frequency of shared clonotypes in human B cell receptor repertoires.
921 *Nature* **566**, 398-402, doi:10.1038/s41586-019-0934-8 (2019).
922 50 Guo, Y., Chen, K., Kwong, P. D., Shapiro, L. & Sheng, Z. cAb-Rep: A Database of Curated
923 Antibody Repertoires for Exploring Antibody Diversity and Predicting Antibody
924 Prevalence. *Front Immunol* **10**, 2365, doi:10.3389/fimmu.2019.02365 (2019).
925 51 Abascal, F., Zardoya, R. & Telford, M. J. TranslatorX: multiple alignment of nucleotide
926 sequences guided by amino acid translations. *Nucleic Acids Res* **38**, W7-13,
927 doi:10.1093/nar/gkq291 (2010).

928 52 Lefranc, M. P. IMGT, the International ImMunoGeneTics Information System. *Cold*
929 *Spring Harb Protoc* **2011**, 595-603, doi:10.1101/pdb.top115 (2011).
930 53 DeWitt, W. S., 3rd, Mesin, L., Victora, G. D., Minin, V. N. & Matsen, F. A. t. Using
931 Genotype Abundance to Improve Phylogenetic Inference. *Mol Biol Evol* **35**, 1253-1265,
932 doi:10.1093/molbev/msy020 (2018).
933